APR 12 1967

INVESTIGATION OF BOUNDARY-LAYER TRANSITION ON SWEPT WINGS AT MACH NUMBERS 2.5 TO 5

By

S. R. Pate and R. E. Brilhart

von Kármán Gas Dynamics Facility

ARO, Inc.

TECHNICAL DOCUMENTARY REPORT NO. AEDC-TDR-63-109

July 1963

AFSC Program Area 750A , Project 1366 , Task 136612

Approved for public release; distribution unlimited.

ARNOLD ENGINEERING DEVELOPMENT CENTER

AIR FORCE SYSTEMS COMMAND

UNITED STATES AIR FORCE

NOTICES

INVESTIGATION OF BOUNDARY-LAYER TRANSITION ON SWEPT WINGS AT MACH NUMBERS 2.5 TO 5

By

S. R. Pate and R. E. Brillhart

von Kármán Gas Dynamics Facility

ARO, Inc.

a subsidiary of Sverdrup and Parcel, Inc.
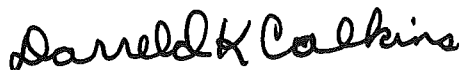
July 1963

ARO Project No. VD0318

ABSTRACT

Tests were conducted in the 12-in. Supersonic Tunnel of the von Kármán Gas Dynamics Facility to determine boundary-layer transition locations on swept wings having a circular arc profile and modified arc profile. Test Mach numbers were from 2.5 to 5 over a Reynolds-number-per-inch range from 0.14 to 1.08 million at sweep angles of 24, 36, and 50 deg for angles of attack of 0 and approximately -4 deg.

Boundary-layer transition Reynolds numbers determined by a pitot probe, and results obtained visually with a sublimable solid are presented. The major factors influencing boundary-layer transition were wing sweep and model leading edge geometry. Increasing wing sweep and leading edge bluntness above a sweep angle of approximately 20 deg decreased the transition Reynolds number at all test Mach numbers.

PUBLICATION REVIEW

This report has been reviewed and publication is approved.

Darreld K. Calkins
Major, USAF
AF Representative, VKF
DCS/Test

Jean A. Jack
Colonel, USAF
DCS/Test

CONTENTS

ILLUSTRATIONS

NOMENCLATURE

b	Wing leading edge thickness, in.
c	Wing chord measured perpendicular to leading edge, (9.45 in.)
LE	Model leading edge
ℓ	Distance parallel to model leading edge, in.
M_∞	Free-stream Mach number
p_o'	Pitot pressure in boundary layer, psia
p_{o_1}'	Local pitot pressure outside boundary layer, psia
p_s	Model surface pressure, psia
p_∞	Free-stream static pressure, psia
Re/in.	Reynolds number per inch
Re_t	Boundary-layer transition Reynolds number determined by sublimation technique, $\left(\frac{\mu}{\nu}\right)_\infty x_t$
$(Re_t)_{Beg.}$	Boundary-layer transition Reynolds number based on beginning-of-transition location as determined by a pitot probe, $\left(\frac{\mu}{\nu}\right)_\infty x_t$
$(Re_t)_{End}$	Boundary-layer transition Reynolds number based on end-of-transition location as determined by a pitot probe, $\left(\frac{\mu}{\nu}\right)_\infty x_t$
$Re_{\Delta x}$	Boundary-layer transition Reynolds number based on length of transition region $\left(\frac{\mu}{\nu}\right)_\infty \Delta x$
T	Temperature, °R
U	Velocity, ft/sec
x	Model coordinates and distance to transition region, which is measured parallel to free-stream, in.
y	Model coordinates and vertical distance above model surface, in.
α	Angle of attack, deg
η_r	Temperature recovery factor $(T_w - T_\delta)/(T_o - T_\delta)$

θ Bevel angle of lower wing leading edge, deg

Λ Wing sweep angle, deg

μ Mach cone angle $(\sin^{-1}\frac{1}{M_\infty})$, deg

ν Kinematic viscosity, $\frac{\text{in.}^2}{\text{sec}}$

SUBSCRIPTS

t   At transition

w   Body surface

δ Edge of boundary layer

∞ Free-stream condition

1.0 INTRODUCTION

Under the sponsorship of the Aeronautical Systems Division (ASD), Air Force Systems Command (AFSC) an investigation of natural boundary-layer transition on swept wings was conducted for the NORAIR Division of Northrop Corporation. Tests were made in the 12-in. Supersonic Tunnel of the von Kármán Gas Dynamics Facility (VKF), Arnold Engineering Development Center (AEDC) AFSC, during the period November 12 to December 20, 1962. Test Mach numbers were 2.5 to 5, at wing sweep angles of 24, 36, and 50 deg over a Reynolds-number-per-inch range from 0.14 to 1.08 million for angles of attack of 0 and approximately -4 deg.

At supersonic speeds, wing sweep is favorable from the viewpoint of reduced wave drag, but unfavorable since sweep can reduce the transition Reynolds number because of cross flows resulting from wing spanwise pressure gradients (Ref. 1) and since sweep reduces the favorable influence on transition resulting from leading edge shock effects (Ref. 2).

Extensive boundary-layer testing has been performed on hollow cylinders and cones (Refs. 3, 4, and 5) with some transition results being obtained on swept flat plates and wings (Refs. 6 and 7). The present investigation was conducted primarily to obtain basic transition measurements on swept wings with cross flows resulting from a spanwise pressure gradient.

2.0 APPARATUS

2.1 WIND TUNNEL

The 12-in. supersonic tunnel (Fig. 1) is an intermittent, variable density wind tunnel with a manually adjusted, flexible plate-type nozzle. The tunnel operates at Mach numbers from 1.5 to 5 at stagnation pressures from about 5 to 60 psia and at stagnation temperatures up to about 100°F. A description of the tunnel and its calibration are given in Refs. 8 and 9.

Manuscript received April 1963.

2.2 MODELS

The NORAIR models, Figs. 2 through 4, were strut-mounted from the tunnel sidewall as shown in Fig. 2b. A spindle was constructed in the mounting strut to rotate the model between sweep angles of 24 and 50 deg, but testing was conducted only at angles of 24, 36, and 50 deg. Changes in angle of attack were facilitated by inserting wedges between the model and mounting strut. Each of the two models tested had a 3-percent thick profile section and were identical in planform and leading edge bevel angle (θ = 11.84 deg), and each was instrumented to measure nine surface pressures (see Fig. 3). Small differences in leading edge thickness existed between the models as shown in the table in Fig. 3, however the major differences existed between the model surface profile geometry up to the 50-percent chord as shown in Fig. 4. Although it was unintentional, the leading edge thickness of the two models varied from 0.006 to 0.009 in. along their wing span as shown in the table in Fig. 3. Each model was constructed of steel and had a surface finish of 3 to 6 microinches rms.

2.3 BOUNDARY-LAYER PROBE

The boundary-layer probe assembly consisted of three separate pitot probes mounted to adjustable carriers that enabled measurement of boundary-layer transition at three wing spanwise locations, as shown in Fig. 5. Each of the probes and probe carriers were identical in construction and the pitot probe tips were approximately elliptical in shape, with inside dimensions of 0.016 by 0.038 in. The probe was mounted to a magnetic head that assured continuous contact between the model surface and the pitot probe as the probes were moved over the wing surface. Another pitot probe was located in the same plane as the boundary-layer probe, but positioned outside the boundary layer and served to furnish a reference pressure. The probe assembly was connected to an automatically controlled electrical drive that provided 7 in. of probe travel and was accurate to within ±0.05 in.

2.4 INSTRUMENTATION

Model data recorded during the test were boundary-layer pitot pressures and model surface pressures. The boundary-layer pitot pressures were measured with small wafer-type transducers (0.58-in. diam by 0.19 in. thick) (see Ref. 8) that were mounted in the probe carrier approximately 5 in. aft of the probe tip, as shown in Fig. 5. The relatively short distance between probe tip and transducer eliminated excessive

lag-time that could have affected the pressure traces. The analog output from the transducers provided traces on X-Y plotters of the pitot pressures as the probe was traversed through the boundary layer along the model surface. Tunnel operating conditions and model surface pressures were automatically recorded and tabulated by the VKF automatic data handling system while the test was in progress.

3.0 METHODS USED TO DETERMINE TRANSITION

Several methods have proved successful in determining the location of boundary-layer transition. Among these are the use of (1) hot wire anemometer, Ref. 3; (2) pitot probe technique, Ref. 3; (3) luminescent lacquer, Ref. 7; (4) sublimation technique, Ref. 6; (5) schlieren pictures; and (6) surface temperature measurements, Ref. 3. The methods used in the present investigation were the pitot probe and the sublimation techniques.

3.1 PITOT PROBE TECHNIQUE

A pitot probe sliding along a model surface and submerged in the boundary layer will produce a pressure trace that is directly related to the boundary-layer velocity profile. The pressure trace, in general, will exhibit both a minimum and maximum point (providing the probe traverses from the laminar to turbulent region) which can be used to locate the end of the laminar region and the beginning of the turbulent region. It has been the experience of the authors and also Potter and Whitfield (Ref. 3) that the beginning of transition, as determined by a pitot probe and defined by the minimum p_0' value, was difficult to obtain on a hollow cylinder, but the end of transition as defined by the maximum p_0' value was very pronounced; however, in the present investigation it was found that both the minimum and maximum p_0' values were well defined as shown in Fig. 9. This is attributed to the fact that the models in the present test subjected the boundary layer to the destabilizing effect of sweep and cross flow, which resulted in a more sharply defined region of transition than occurred on the hollow cylinder model.

To determine if transition varied along the wing span, three pitot probes were used simultaneously as shown in Fig. 5. Spanwise locations of the probes varied with sweep angle to provide maximum model surface coverage with the minimum amount of interference from the wing tips, as shown in Fig. 6.

3

3.2 SUBLIMATION TECHNIQUE

Visual indication of boundary-layer transition by the use of a volatile chemical solid as a diffusible coating film is a simple and relatively easy process. A solution of the indicating substance (diffusible solid) and a suitable solvent, is sprayed on the model and within a period of time the chemical coating in the turbulent region will sublimize, leaving the coating in the laminar region clearly visible. A complete coverage of chemical solids for indicating materials in determining boundary-layer transition is provided by Main-Smith in Ref. 10.

A saturated solution of naphthalene (diffusible solid) and petroleum ether (solvent) has been used successfully to locate transition at supersonic speeds, Ref. 6, but for the investigations in the VKF 12-in. supersonic tunnel, the use of naphthalene as the indicating material did not produce satisfactory results. Before tunnel starting, the tunnel was evacuated to a low pressure (lasting approximately 2 min.) and because of the high volatility of naphthalene, sublimation usually occurred before flow was established. Rygh and Martin (Ref. 11) used azobenzene as the the sublimable solid with a tunnel running time of several minutes (time $\approx$ 60 min for $T_O = 70°F$, $M_\infty = 3$) required for transition indication. Based on their results and the experience in the present tests with naphthalene, it was found that a saturated solution of naphthalene and petroleum ether with approximately 2 percent azobenzene (by weight) produced satisfactory results. Transition indications occurred approximately 1 to 2 min after flow was established.

After a test run the transition line was clearly visible and transition locations were measured directly at the three spanwise stations corresponding to the probe locations. The transition line was then traced with ink and photographed. Some photographs were also taken during tunnel operation.

4.0 PROCEDURE

Testing was conducted at the following conditions:

Configuration	M_∞	Re/in. x 10^{-6} Max	Re/in. x 10^{-6} Min	α, deg	Λ, deg	Methods of Measurement
Circular Arc	2.5	1.08	0.34	0, -4.2	24, 36, 50	Probe
Circular Arc	3.0	0.81	0.26	0, -4.2	24, 36, 50	Measurements
Modified	3.0	0.81	0.26	0, -4.6	24, 36, 50	
Circular Arc	4.0	0.50	0.16	0, -4.2	24, 36, 50	
Modified	4.0	0.50	0.16	0, -4.6	24, 36, 50	
Circular Arc	5.0	0.30	0.14	0, -4.2	50	
Modified	5.0	0.30	0.14	0, -4.6	50	
Circular Arc	2.5	1.06	-	0	36	Sublimable Solid
Circular Arc	3.0	0.81	0.27	0, -4.2	24, 36, 50	
Modified	3.0	0.81	0.27	0, -4.6	50	
Circular Arc	4.0	0.48	0.24	0, -4.2	36, 50	
Modified	4.0	0.48	0.24	0, -4.6	36, 50	
Circular Arc	5.0	0.29	-	-4.2	36	

4

Before each test run, the model was inspected for leading edge or model surface discontinuities that might have resulted from the probe assembly. Transition measurements were obtained by traversing the three probes in both directions on the model surface, and as seen in Figs. 9 and 10, there was no appreciable difference in the respective traces.

5.0 RESULTS AND DISCUSSION

5.1 TEST PARAMETERS

Parameters investigated were wing sweep, Mach number, unit Reynolds number, model surface curvature, and small changes in angle of attack. No effort was made to control model temperature. The tunnel stagnation temperatures varied from 40 to 80°F during the test, but were essentially constant during a particular tunnel pressure level. Dunning and Ulmann (Ref. 7) found that an equilibrium temperature on wing models of comparable size to the models in the present investigation and with equivalent tunnel stagnation temperatures was reached after approximately 80 sec of running time. Most of the runs in the VKF test were from 1 to 10 min and consequently, the models were probably at an equilibrium temperature. For these reasons and the fact that the variations in stagnation temperature produced no noticeable effect on transition locations, the temperature was considered of secondary importance.

5.2 MODEL SURFACE PRESSURES

Presented in Fig. 7 are the experimental and theoretical surface pressure distributions on the circular arc profile model for $M_\infty = 2.5$ and 4, $\alpha = 0$ and -4.2 deg and three sweep angles. The theoretical results are for the shock expansion method and are in good agreement with the experimental data. The differences in the spanwise pressures at $M_\infty = 2.5$, $\alpha = -4.2$ for $\Lambda = 50$ deg can be explained by referring to Fig. 6c where it may be noted that some of the orifices are within the influence of the Mach cone emanating from the wing tip. Differences also existed in the experimental spanwise pressures at $M_\infty = 4$, $\alpha = -4.2$ and $\Lambda = 50$ deg, but only one orifice was within the Mach cone region and, consequently, the reason for the other scatter is unknown.

The experimental surface pressures obtained on the modified arc profile model and the corresponding theoretical distributions are presented in Fig. 8 for $M_\infty = 3$ and 4. These data follow closely the pattern

5

exhibited by the circular arc profile data and scatter in the spanwise data at Λ = 50 deg can in part be explained by the reasons given previously.

5.3 TRANSITION RESULTS – PITOT PROBE TECHNIQUE

Typical pressure traces obtained by pitot probes moving along the model surface are presented in Figs. 9 and 10 for Mach numbers 3, 4, and 5. As seen from these traces the minimum and maximum values that define the beginning and end of boundary-layer transition were, in general, very distinct. Also presented for comparison are some transition locations as determined using the sublimation technique.

Flow entering a turbulent region does not remain in laminated layers with smooth streamlines, which is typical of laminar flow, but fluctuates and causes a transfer of energy between streamlines. It is of interest to observe in Fig. 10 that the pitot pressure traces were relatively smooth in the laminar region, but upon entering the transition region the traces show a fluctuation that continued into the fully developed turbulent region.

It was not known for certain that an absolute value of the pitot pressure in the boundary layer near the model surface would provide the best indication of transition. Therefore, a second pitot probe (p_{o_1}') was located directly above the boundary-layer probe but was positioned outside the boundary layer (see Fig. 11a) to provide a reference pressure to the boundary-layer probe transducer. A typical pressure trace ($p_{o_1}' - p_{o}'$) with this system is shown in Fig. 11a. The pitot pressure trace in Fig. 11b was obtained under identical tunnel conditions as the trace in Fig. 11a, but with a vacuum reference pressure (50 microns Hg). It is understood that the use of a pitot probe reference pressure in place of a vacuum reference will reverse the pressure trace as shown by Figs. 11a and 11b. The maximum and minimum points are located at x_t = 3.6 in. and x_t = 4.0 in. in Figs. 11a and 11b, respectively, and suggest that the pitot pressure traces do not give a consistent location for the beginning of transition.

It should be noted that when locating transition on a curved surface using the absolute pitot pressure, the varying surface pressure must be considered when defining the transition location. For some of the tests, the transducer reference pressure was supplied by a pitot probe which moved over the wing surface at a position outside of the boundary layer. Since the reference pressure varied because of the local Mach number, these variations must also be considered when defining the transition location. The procedures used to define the location of transition using a vacuum or pitot pressure for a reference are shown in Figs. 11a and 11b.

6

Figure 11c presents the beginning-of-transition Reynolds number for M_∞ = 3, Λ = 24 deg, and α = 0 as determined with a pitot pressure reference, a vacuum reference, and the peak or minimum point on the pitot pressure trace. The same data determined with the slope correction (Fig. 11d) show that the correction procedure used provided consistent results. Although the trace in Fig. 11a was very distinct, not all traces obtained using a pitot pressure reference produced satisfactory results, especially at the higher Mach numbers, and, therefore, most of the probe transition data were obtained using a vacuum reference.

Beginning-of-transition results obtained with pitot probes on the circular arc and modified arc profile models are presented in Figs. 12 and 13 for M_∞ = 2.5 to 5, Λ = 24, 36, and 50 deg, α = 0 and approximately -4 deg for varying unit Reynolds number and three wing spanwise locations. These data exhibit the usual linear variation with unit Reynolds number as was shown by Potter and Whitfield (Ref. 3), for a hollow cylinder. Also, clearly indicated is a large decrease in transition Reynolds number with increased wing sweep. A very noticeable difference is also seen to exist between spanwise rake locations, with the general trend being a decrease in transition Reynolds number with increasing wing span (No. 1 to No. 3 probe). The one exception being the center probe (No. 2) data obtained on the circular arc profile at M_∞ = 3, α = 0, and Λ = 24 deg. These low transition Reynolds numbers could be the result of a small indentation that was located at the leading edge, ℓ = 7.1 in., on the underside of the wing. It should be noted that the results for the modified circular arc profile model at the same conditions do not show this inconsistency.

Potter and Whitfield (Ref. 3) determined a correlation equation for transition Reynolds numbers on a hollow cylinder at M_∞ = 3 which accounts for unit Reynolds number and leading edge geometry. Their results were used to estimate the beginning-of-transition Reynolds numbers for M_∞ = 3, Λ = 0 at α = 0 which are presented in Figs. 12c and 13d.

The tests were conducted at negative angles of attack so that the leading edge angles for the upper and lower surfaces were equal. This eliminated the possibility of any adverse effects resulting from airflow around the leading edge from the high pressure lower surface that might otherwise have occurred at α = 0. A comparison between the α = 0 and approximately -4 deg data in Figs. 12 and 13 will show that the change in angle of attack produced no significant differences in the transition Reynolds numbers.

A direct comparison is made in Fig. 14 between the transition results obtained on the circular arc and modified arc profile for M_∞ = 3 and 4 and α = 0. The Reynolds number based on the distance to the

7

end of transition did not exhibit the same linearity as the beginning-of-transition results and the linearity and unit Reynolds number effect generally decreased with increasing sweep. Although there was considerable difference between the surface curvature for the circular arc and modified arc models, the transition results show only small effects of profile geometry at $M_\infty = 3$ and no effects at $M_\infty = 4$. This indicates that at a given Mach number the leading edge geometry and sweep angle were the governing parameters influencing transition.

5.4 TRANSITION RESULTS – SUBLIMATION TECHNIQUE

Boundary-layer transition as determined by a sublimable solid produced patterns similar to the results presented in Fig. 15 for $M_\infty = 3$, $\Lambda = 24$ deg, $\alpha = 0$, and Re/in. $= 0.81 \times 10^6$. The photograph in Fig. 15a was taken during tunnel operation and clearly illustrates the laminar and turbulent regions of the boundary-layer. Figure 15b presents the same data, but with the transition line traced with ink after tunnel shutdown.

Presented in Fig. 16 are transition photographs (with ink trace) for $M_\infty = 3$, $\Lambda = 36$ and 50 deg, $\alpha = 0$, and several unit Reynolds number ranges. Transition results obtained with the pitot probes indicated that transition Reynolds number decreased with increasing wing span. The photographs in Figs. 15 and 16 also show a decrease in transition distance with increasing wing span.

To be certain that the sublimable solid remained on the model surface only in the laminar region and to verify what appeared to be the transition line, a roughness particle was glued on the model surface near the leading edge. The particle produced a turbulent streak in the laminar region and indicated without question that the sublimable solid was giving correct indications of boundary-layer transition.

The transition results obtained by the sublimation technique at the No. 2 probe location are presented in Fig. 17 for $M_\infty = 2.5$ to 4. It is of interest to note that the variations in transition Reynolds number with unit Reynolds number are not linear as are the beginning-of-transition results obtained with the pitot probe, but exhibit trends similar to the end-of-transition results.

Sublimation results show that transition is forward of the end-of-transition located by the pitot probe technique. Rygh and Martin (Ref. 11) found that transition locations as determined by a sublimable solid (azobenzene) were approximately equal to or slightly forward of locations determined by surface temperature results. Potter and Whitfield's study (Ref. 3) on a hollow cylinder shows that transition as determined

by surface temperature distributions was approximately 86 percent of the end-of-transition values determined by a pitot probe. Figure 18a presents a comparison between end-of-transition results obtained by pitot pressure measurements and transition results determined from surface temperatures and a sublimable spray. Transition located by the sublimable spray was approximately 20 percent forward of the location obtained with the pitot probe technique at Mach 2.5 to 5. Shown in Fig. 18b is a typical temperature recovery profile obtained on a hollow cylinder (Ref. 3) at $M_\infty = 3.5$, Re/in. $= 0.27 \times 10^6$. Also shown for general comparison is the range of transition locations as determined by the sublimable spray.

5.5 TRANSITION REGION

It is a well-known fact that the boundary-layer transition from laminar to turbulent flow does not occur instantaneously at a particular location, but over a distance of many boundary-layer thicknesses as is shown in Figs. 9 through 11. Potter and Whitfield (Ref. 3) observed that a Reynolds number based on the transition zone length ($Re_{\Delta x}$) was fairly independent of leading edge geometry and unit Reynolds number and dependent on Mach number and the transition Reynolds number. Results from Ref. 3 are presented in Fig. 19 for Mach number zero to 4.5. Data obtained in the present investigation are shown for $M_\infty = 2.5$, 3, and 4 and several unit Reynolds numbers. These data were not independent of unit Reynolds number and did not, in general, follow the curves of Ref. 3 but indicate that perhaps at the lower unit Reynolds numbers they approach the curves for $M_\infty \cos \Lambda$. Although these data are not in complete agreement with the results from Ref. 3 it must be remembered that the end-of-transition results did not have a linear variation with unit Reynolds number as did the correlation curves obtained on the hollow cylinder, and also increased sweep had an increasing detrimental effect on transition and consequently had a pronounced effect on the length of the transition zone.

5.6 EFFECT OF MACH NUMBER

The influence of Mach number on transition Reynolds number is presented in Fig. 20 for three sweep angles and Re/in. $= 0.50 \times 10^6$. The transition Reynolds number curves having a minimum value between $M_\infty = 3$ and 4 are common type results that have been observed by Laufer and Marte (Ref. 4) and Potter and Whitfield (Ref. 3). The hypothesis was made by Moeckel (Ref. 2) that transition Reynolds numbers based on local conditions are unchanged when a sharp leading edge is blunted. This leads to the conclusion that the location of transition is inversely

proportional to the ratio of local surface unit Reynolds number behind a blunted leading edge to the unit Reynolds number of an "aerodynamically" flat plate (b→0). Using the equations in Ref. 6, which were based on Moeckel's hypothesis, the effects of free-stream Mach number on boundary-layer transition were determined. This equation gives only the rate of change of transition Reynolds number with Mach number, and, therefore, the predicted transition Reynolds number is assumed equal to the experimental value at $M_\infty = 4$. As shown in Fig. 20b, the increase in transition Reynolds number with increased Mach number as predicted by Moeckel (Ref. 2) was in agreement with experimental results above $M_\infty \approx 3.5$.

5.7 EFFECT OF SWEEP

Variations in the normalized transition Reynolds number $(Re_t)_\Lambda / (Re_t)_{\Lambda = 0}$ with wing sweep are presented in Fig. 21 for $M_\infty = 2.5, 3,$ and 4 for a unit Reynolds number of 0.50×10^6. The transition values for zero sweep, $(Re_t)_{\Lambda = 0}$, were estimated from Fig. 20 for $M_\infty = 2.5$ and 4 and determined from the Potter-Whitfield correlation (Ref. 3) for $M_\infty = 3$. The $M_\infty = 3$ results include data from the three spanwise locations and illustrate how the effect of increased leading-edge blunting accentuated the decrease in transition Reynolds number with sweep.

Following Moeckel's hypothesis (Ref. 2) that slight blunting would have a favorable effect on transition Reynolds number, Jillie and Hopkins (Ref. 6) developed equations for normalized transition Reynolds number variation with sweep for a flat plate. These theoretical curves presented in Fig. 21 for $M_\infty = 2.5, 3,$ and 4 show that the trends exhibited by the theoretical curves were very similar to the experimental data, with improved agreement occurring with increasing Mach numbers.

Presented in Fig. 22 are the variations in the normalized transition Reynolds number with sweep as determined by the sublimation technique at $M_\infty = 3$ and $Re/in. = 0.60 \times 10^6$. Also presented are the flat plate theoretical predictions and the experimental results obtained by Jillie and Hopkins (Ref. 6) using a sublimable spray on a flat plate. It should be noted that the results for a leading edge thickness of 0.001 are higher than the theoretical prediction and according to Ref. 6 might be explained on the basis that the 0.001-in. thickness was insufficient to produce the full bluntness effect required by the theory for maximum leading edge shock effects.

The reason that sweep on the flat plate had a larger detrimental effect for b = 0.005 in. than the shock loss predictions was believed by

10

Jillie and Hopkins (Ref. 6) to be related to cross-flows that develop over the finite leading edge of swept wings as explained by Chapman in Ref. 1. Photographs obtained by Jillie and Hopkins (Ref. 6) produced evidence of longitudinal vortices, resulting from cross-flow that developed at the leading edge, at all sweep angles except zero. Figure 22 clearly illustrates that the trends exhibited by the flat plate normalized transition Reynolds number with sweep were also present in the VKF investigation. Although these comparisons appear to indicate that the only difference between the data for the two tests was the increase in leading edge thickness, it must be remembered that there was a large difference in unit Reynolds number, which may or may not have had an effect.

5.8 EFFECT OF LEADING EDGE THICKNESS IN CONJUNCTION WITH SWEEP

Transition results for Λ = 24, 36, and 50 deg obtained by the pitot probe and sublimable spray techniques produced evidence of a definite decrease in transition Reynolds number with increasing wing span. Potter and Whitfield (Ref. 3) and Brinich and Sands (Ref. 5) have shown that a small amount of leading edge blunting on a hollow cylinder will increase the transition Reynolds number, however, results from this investigation have shown that although the leading edge thickness increased from 0.006 to 0.008 in. along the wing span (see Fig. 2) there was a corresponding decrease in transition Reynolds number. Transition Reynolds numbers obtained from the present investigation for M_∞ = 3, Re/in. = 0.40 x 10^6 and transition results from Ref. 6 for M_∞ = 3, Re/in. = 1.25 x 10^6 are presented in Fig. 23 for various sweep angles and several leading edge thicknesses. These data show explicitly that at zero sweep angle small amounts of blunting had a favorable effect on transition, but with increasing sweep this favorable effect decreased and above approximately 20 deg becomes detrimental to transition Reynolds number. This adverse effect caused by increased blunting in conjunction with sweep is believed to be the result of cross-flows over the wing leading edge. These cross-flows may have also produced vortex formations that originated at the leading edge (Ref. 1) and which Jillie and Hopkins (Ref. 6) found to exist on blunted flat plates at all sweep angles except zero.

6.0 CONCLUDING REMARKS

Tests were conducted at Mach numbers 2.5, 3, 4, and 5 to investigate the effects of unit Reynolds number, sweep, and model surface

profile on natural boundary-layer transition. On the basis of these investigations the following conclusions are made:

1. At all Mach numbers, the effect of increasing wing sweep (Λ = 24 to 50 deg) was to reduce transition Reynolds numbers.

2. Unintentionally, the leading edge of both wings increased in thickness from 0.006 to 0.008 in. along the span. This resulted in a decrease in transition Reynolds numbers with increased blunting at sweep angles of 24, 36, and 50 deg and all Mach numbers.

3. The major factors influencing boundary-layer transition were wing sweep and leading edge geometry rather than cross-flows developing along the wing chord as a result of spanwise pressure gradients.

REFERENCES

1. Chapman, Gary T. "Some Effects of Leading-Edge Sweep on Boundary-Layer Transition at Supersonic Speeds." NASA Technical Note D-1075, Sept. 1961.

2. Moeckel, W. E. "Some Effects of Bluntness on Boundary-Layer Transition and Heat Transfer at Supersonic Speeds." NACA Report 1312, 1957.

3. Potter, J. Leith and Whitfield, Jack D. "Effects of Unit Reynolds Number, Nose Bluntness, and Roughness on Boundary-Layer Transition." AEDC-TR-60-5, March 1960.

4. Laufer, John and Marte, Jack E. "Results and a Critical Discussion of Transition-Reynolds-Number Measurements on Insulated Cones and Flat Plates in Supersonic Wind Tunnels." Jet Propulsion Laboratory, California Institute of Technology, Report No. 20-96, November 30, 1955.

5. Brinich, Paul F. and Sands, Norman. "Effect of Bluntness on Transition for a Cone and a Hollow Cylinder at Mach 3.1." NACA Technical Note 3979, May 1957.

6. Jillie, Don W. and Hopkins, Edward J. "Effects of Mach Number, Leading-Edge Bluntness, and Sweep on Boundary-Layer Transition on a Flat Plate." NASA Tech. Note D-1071, September 1961.

7. Dunning, Robert W. and Ulmann, Edward F. "Effects of Sweep and Angle of Attack on Boundary-Layer Transition on Wings at Mach Number 4.04." NACA Tech. Note 3473, August 1955.

8. Test Facilities Handbook (4th Edition) "von Kármán Gas Dynamics Facility, Vol. 4." Arnold Engineering Development Center, July 1962.

9. Anderson, A. "Summary Report on Calibration of Tunnel E-1 A 12-Inch Mach 5 Supersonic Wind Tunnel." AEDC-TN-58-8, March 1958.

10. Main-Smith, J. D. "Chemical Solids as Diffusible Coating Films for Visual Indication of Boundary-Layer Transition in Air and Water." Aeronautical Research Council (Gt. Brit.) R and M, 2755, ARC-TR-13, 115, Feb. 1950.

11. Rygh, Patrick J., and Martin, Robert E. "The Use of Azobenzene to Provide a Visual Indication of Supersonic-Boundary-Layer Transition." Jet Propulsion Laboratory, California Institute of Technology, Progress Report No. 20-335, October 15, 1957.
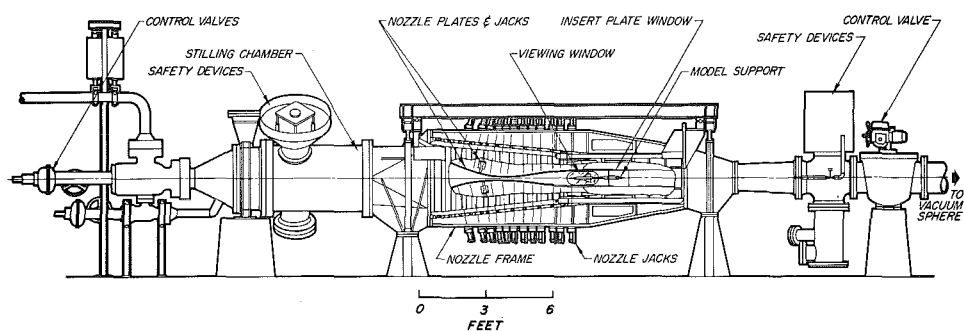
Assembly
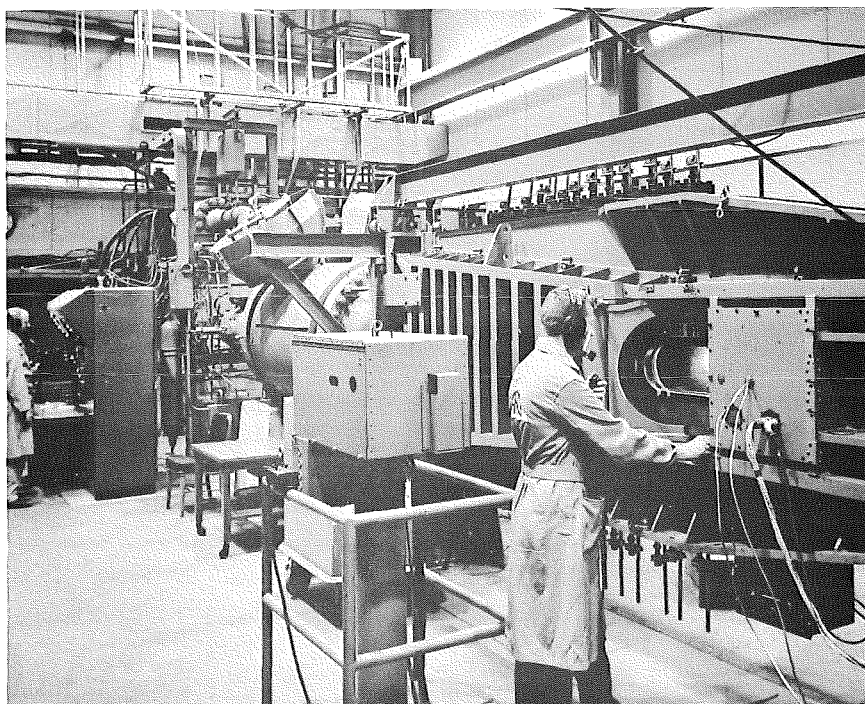
Fig. 1 The 12-Inch Supersonic Tunnel (D)
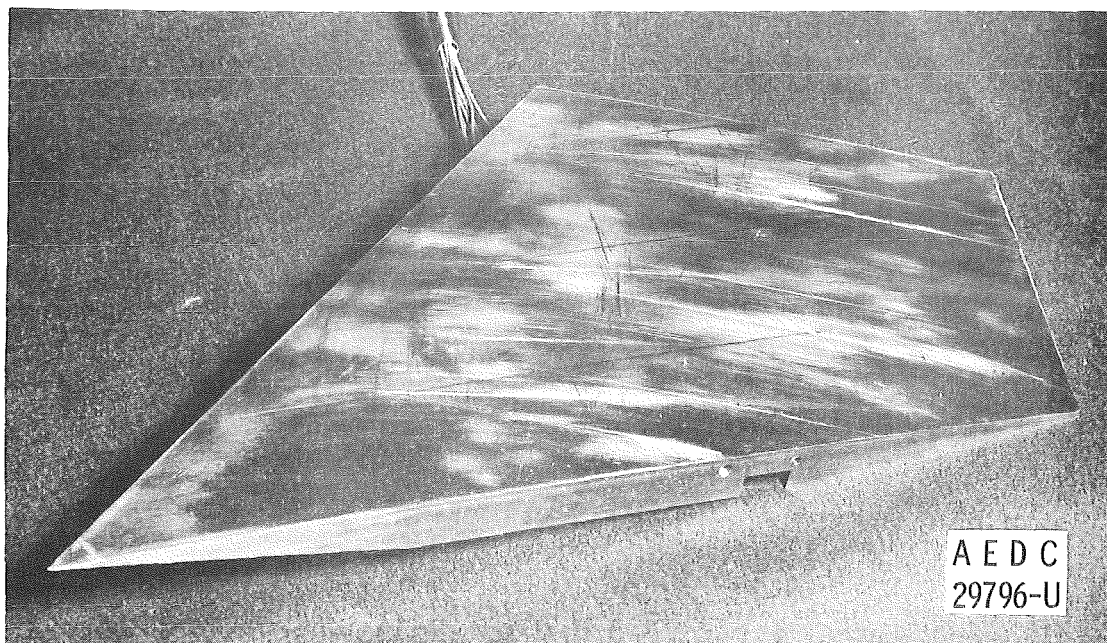
a. Model
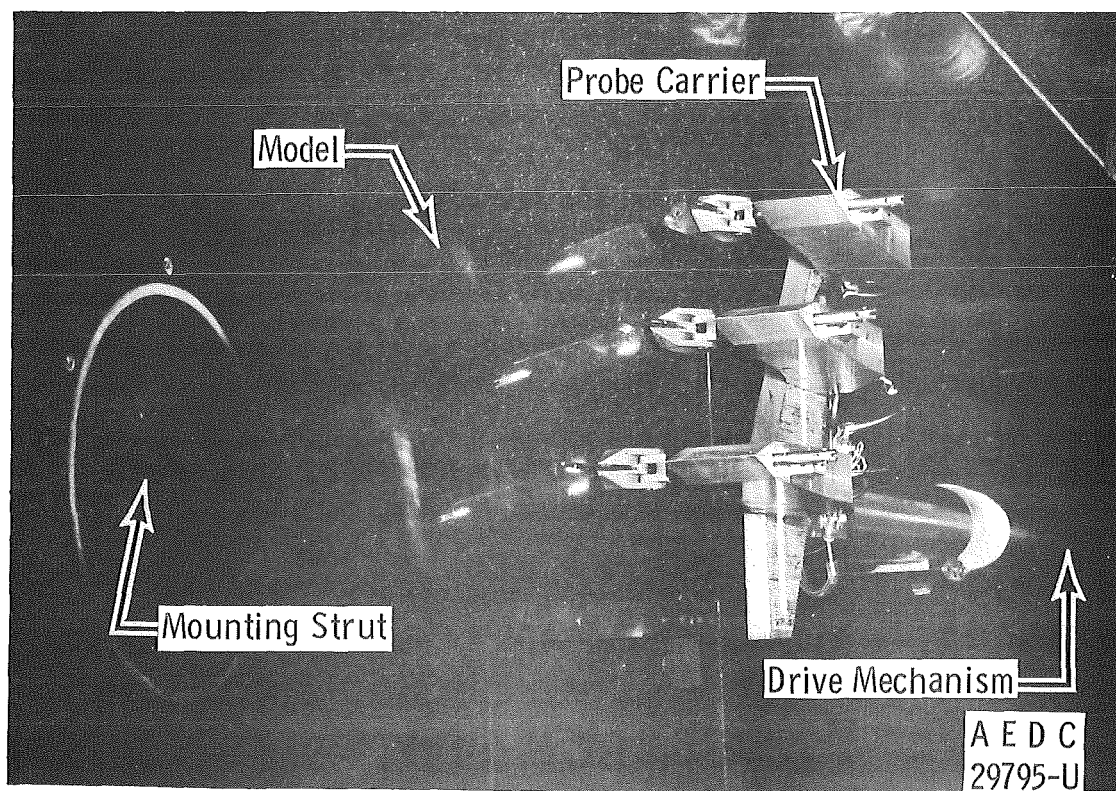
b. Model Installation

Fig. 2 Model Photographs

16

Flow →

0.58 — 0.30

6.34

9.19

2.36

0.94

3.78

A

102 deg

2 Equal
Spaces
(Typical)

114 deg

3.95

12.09

LE

104 deg

A

Mounting Strut

100 Percent Chord
(c = 9.45)

All Dimensions in Inches

2.00

40 deg

ℓ

θ = 11.84 deg

B

0.64

Section A-A

b

Sta. No. 7

View B
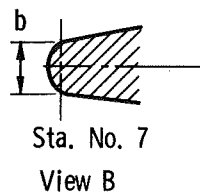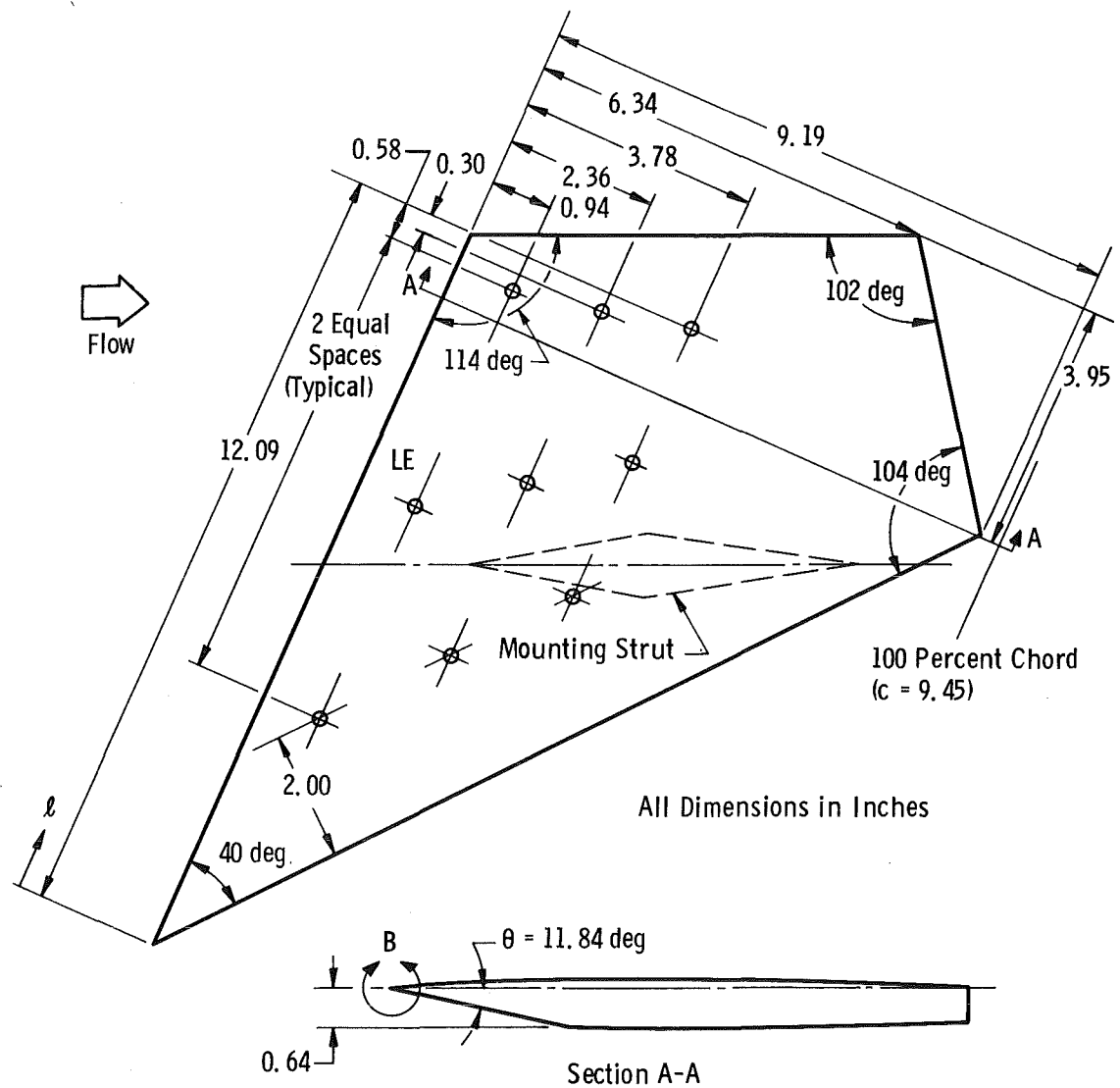
	Circular Arc		Mod. Arc
Sta.	ℓ, in.	b, in.	b, in.
1	2.0	0.0060	0.0060
2	4.0	0.0060	0.0065
3	5.5	0.0060	0.0070
4	7.0	0.0070	0.0070
5	8.5	0.0075	0.0070
6	10.0	0.0080	0.0075
7	11.0	0.0090	0.0080

Fig. 3 Model Geometry

x, in. ⊥ to L E	Circular Arc Profile y, in.	Modified Arc Profile y, in.
0	0	0
0.094	0.0056	0.0042
0.188	0.0111	0.0085
0.284	0.0165	0.0127
0.378	0.0218	0.0170
0.472	0.0270	0.0212
0.566	0.0320	0.0255
0.709	0.0393	0.0319
0.945	0.0510	0.0425
1.417	0.0723	0.0647
1.890	0.0907	0.0844
2.382	0.1063	0.1020
2.835	0.1190	0.1161
3.307	0.1290	0.1272
3.780	0.1360	0.1353
4.252	0.1403	0.1401
4.725	0.1418	0.1418
5.198	0.1403	0.1401
5.670	0.1360	0.1353
6.143	0.1290	0.1272
6.615	0.1190	0.1161
7.088	0.1063	0.1020
7.560	0.0907	0.0844
8.033	0.0723	0.0647
8.505	0.0510	0.0425
8.741	0.0393	0.0319
8.884	0.0320	0.0255
8.978	0.0270	0.0212
9.072	0.0218	0.0170
9.166	0.0165	0.0127
9.262	0.0111	0.0085
9.356	0.0056	0.0042
9.450	0	0

End of Straight Section for Modified Arc Profile (at x = 1.417)
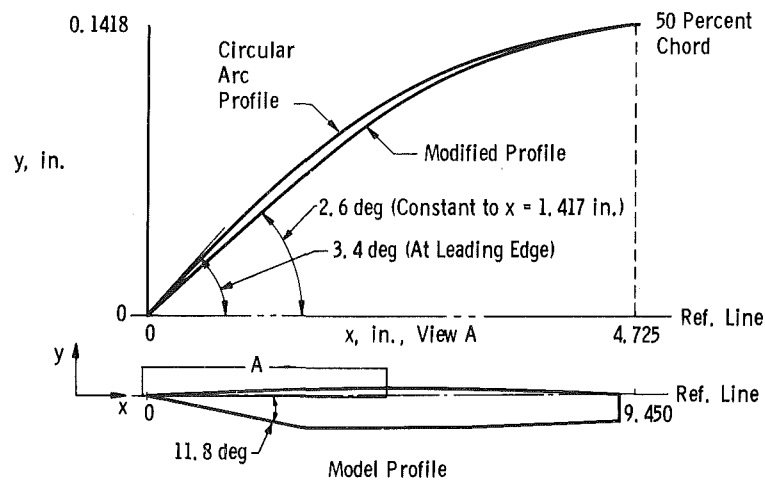
Fig. 4 Model Profile Dimensions

18

Tunnel Wall

Serrations (Typ)

Approx. 5 (Typ)

Alignment Slots (Typ)

Flow

Adjustable Carrier (Typ)

Drive Mechanism

Tunnel ₵

Model

28 deg
(Typ)

A

8.77 (Typ)

0.81 (Typ)

Differential Transducer
3 Places (Typ)

Tunnel Wall

1.37

B

Magnetic
Head

View A

All Dimensions in Inches

0.038

0.80

0.072 OD

0.016

0.004

0.042 OD

View B
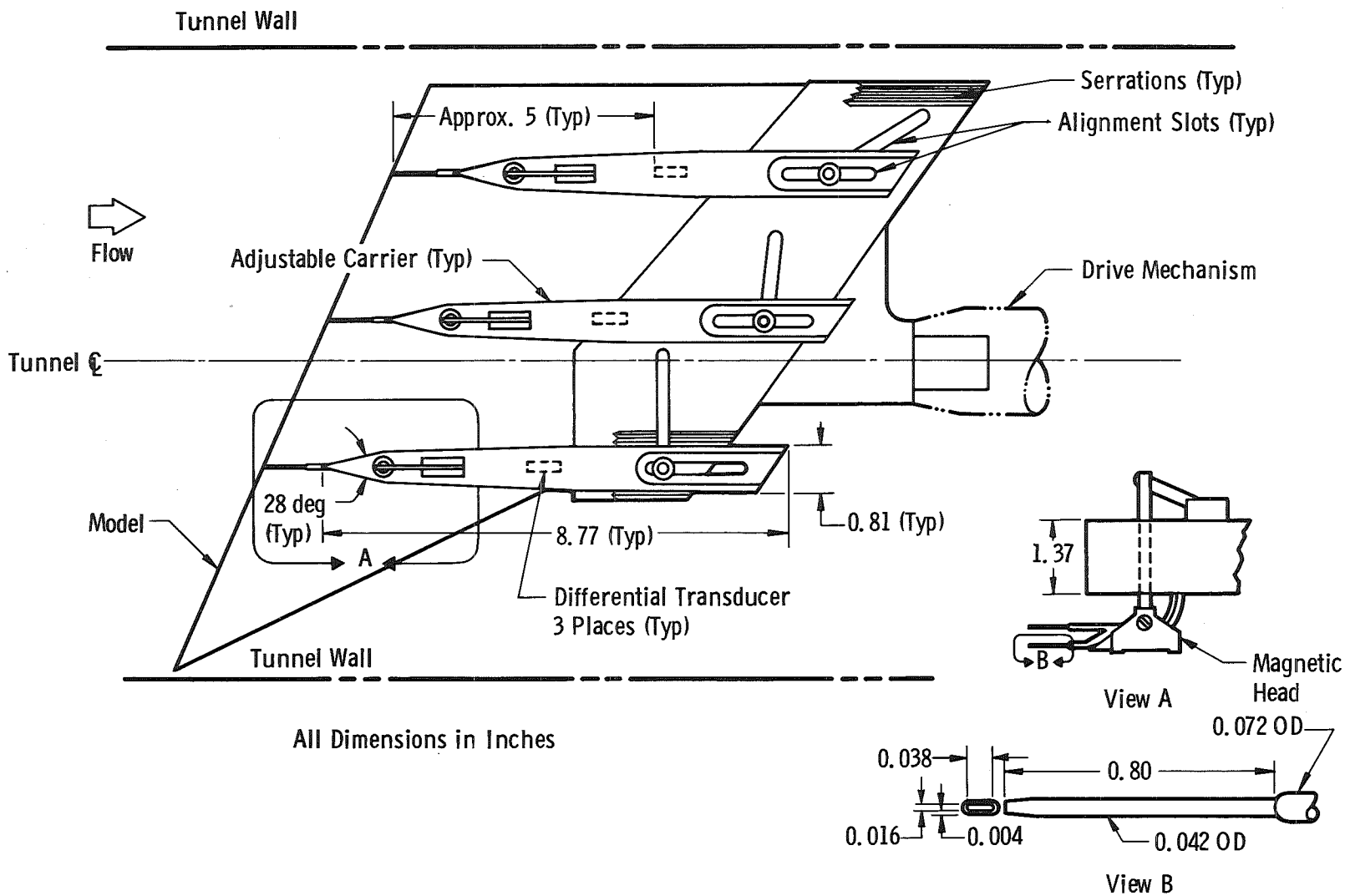
Fig. 5 Sketch of Boundary-Layer Probe Assembly

The 0.50 percent chord was chosen
as the maximum aft boundary-layer
transition distance to be of interest.

a. Λ = 24 deg

b. Λ = 36 deg

c. Λ = 50 deg
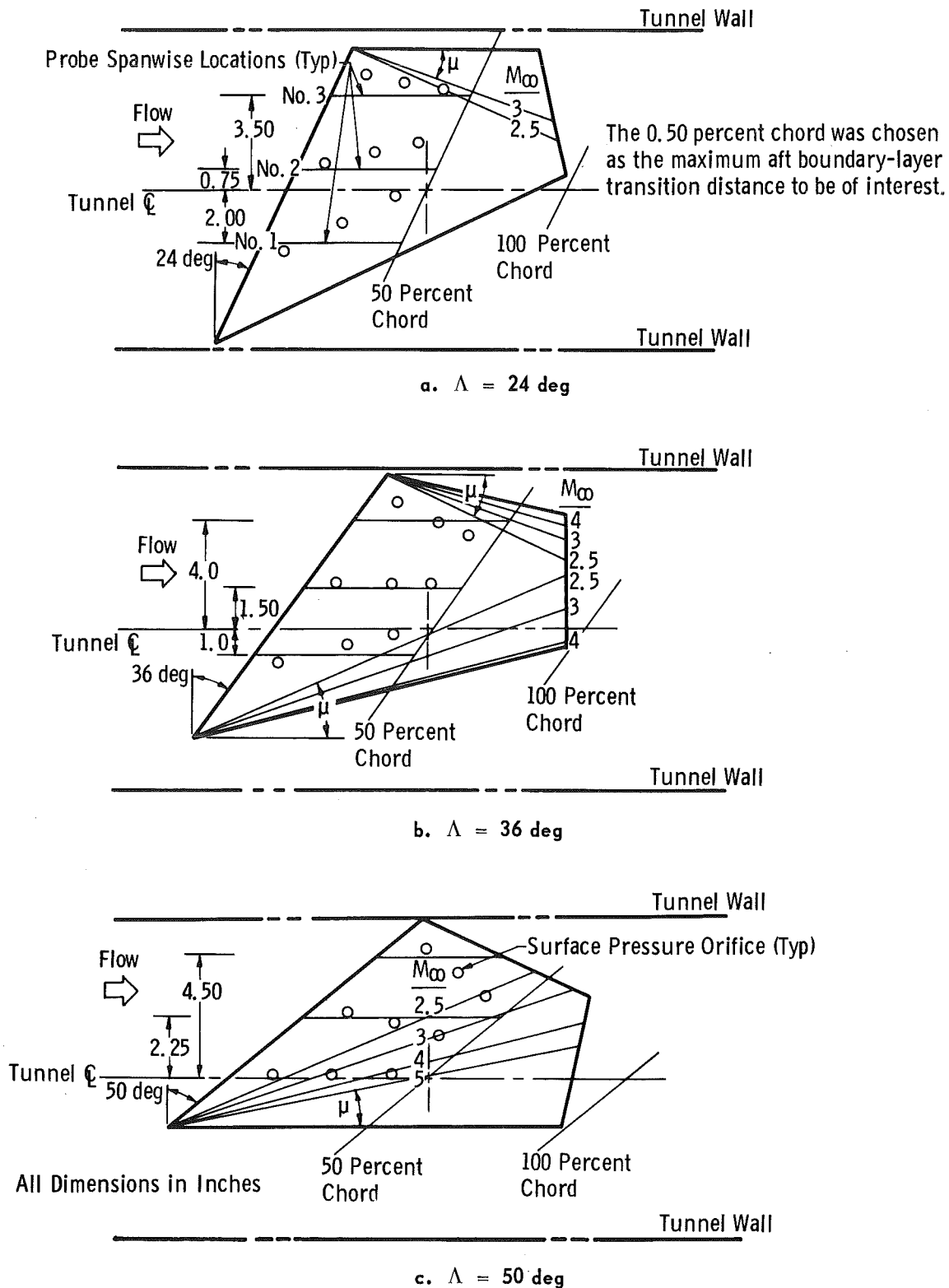
Fig. 6 Sketch Showing Probe Spanwise Locations and Model Surface Areas Exposed to
Tip Effects for Various Mach Numbers and Sweep Angles (Λ)
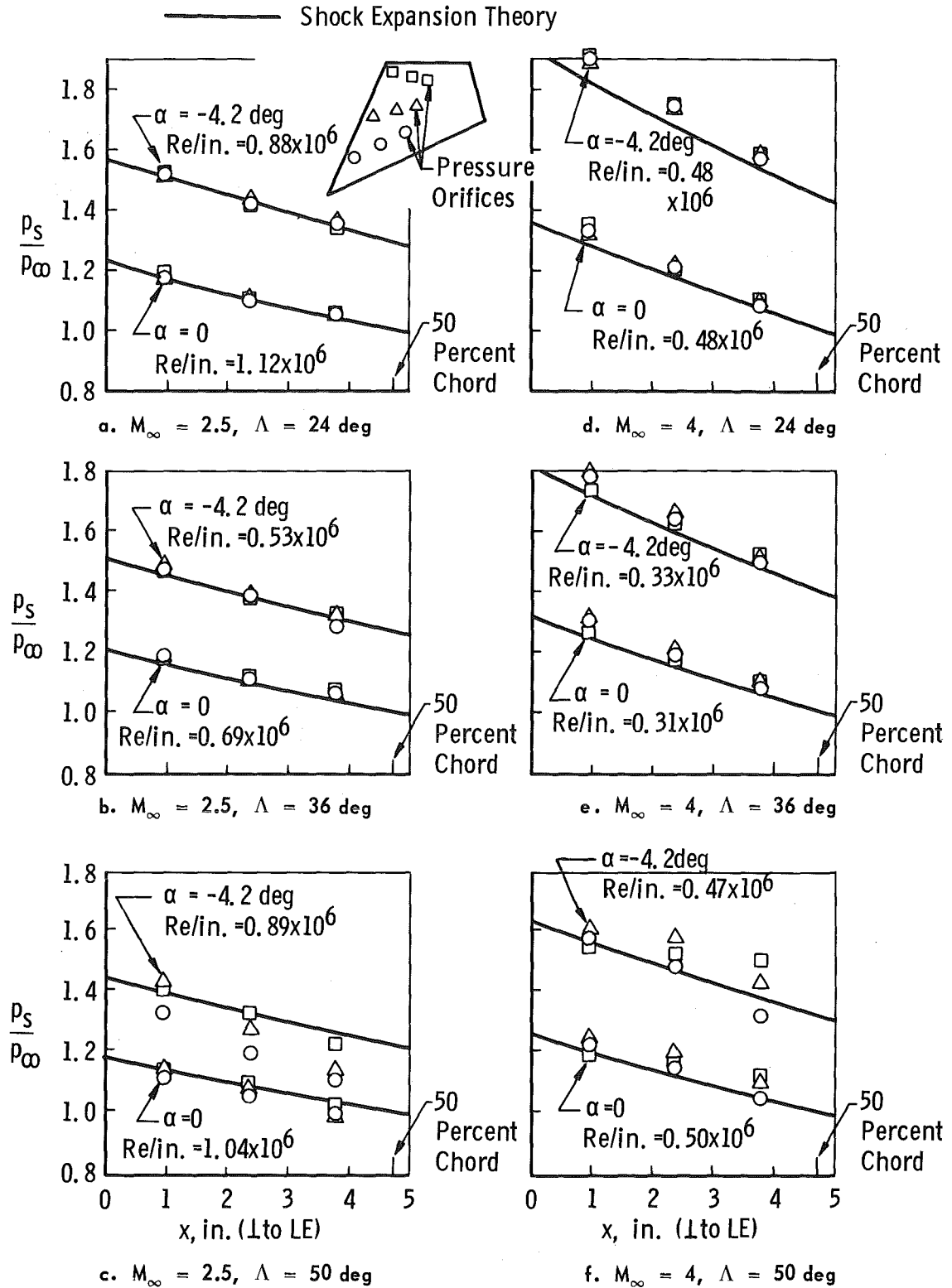
Fig. 7 Surface Pressure Distribution on Circular Arc Profile Model at M_∞ = 2.5 and 4,
α = 0 and −4.2 deg, and Sweep Angles (Λ) of 24, 36, and 50 deg
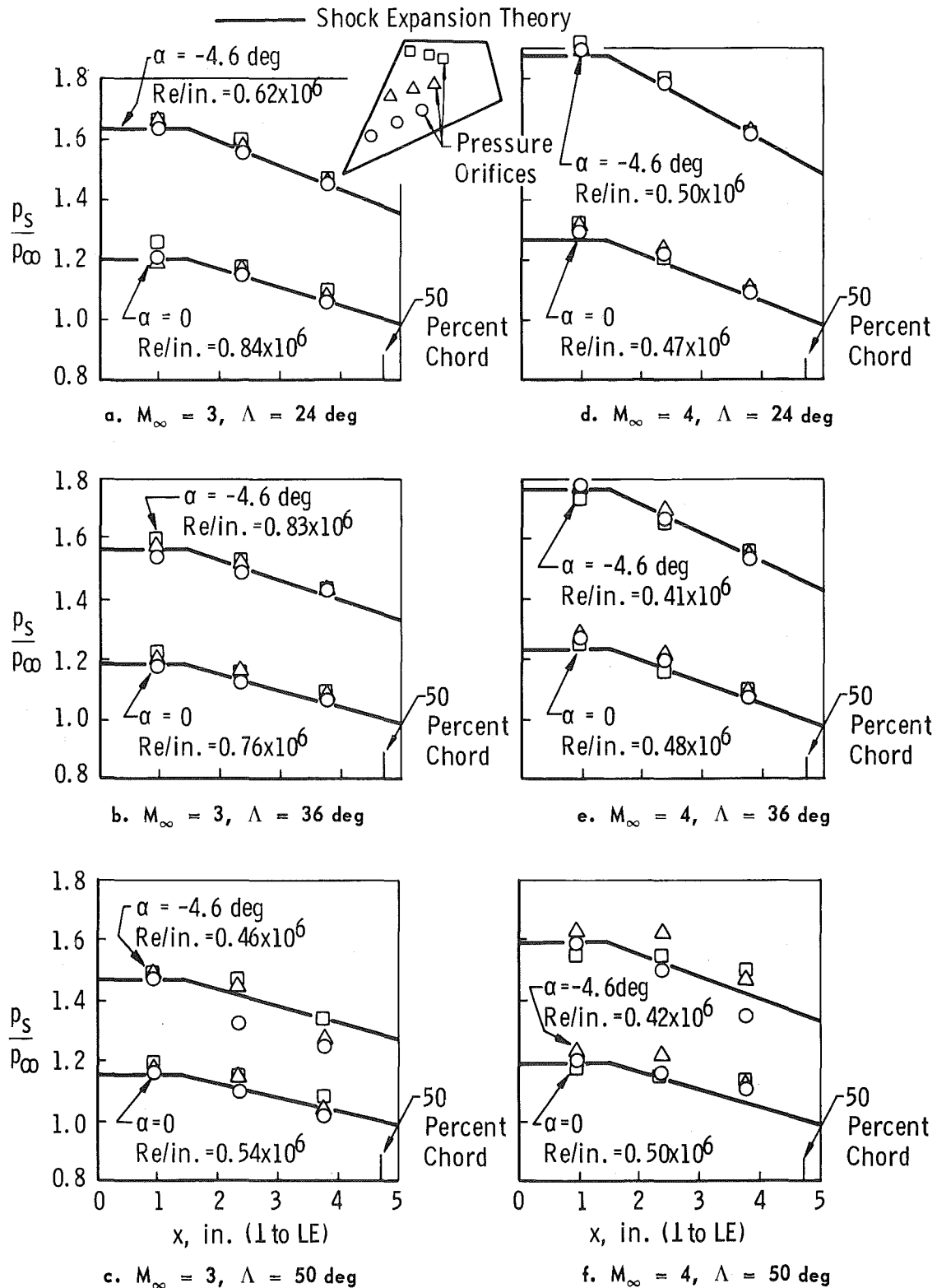
Fig. 8 Surface Pressure Distribution on Modified Arc Profile Model at M_∞ = 3 and 4, α = 0 and −4.6 deg, and Sweep Angles (Λ) of 24, 36, and 50 deg
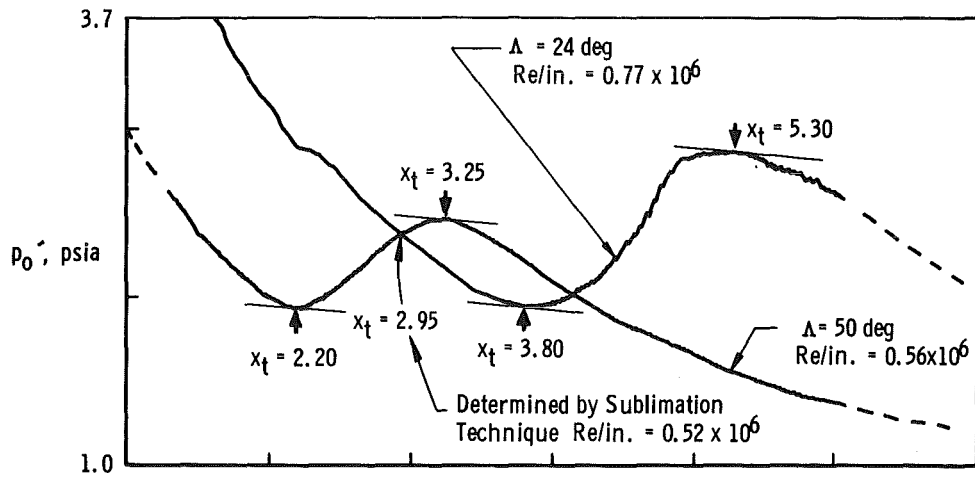
a. Probe No. 1, $M_\infty = 3$, $\Lambda = 24$ and 50 deg, $a = 0$
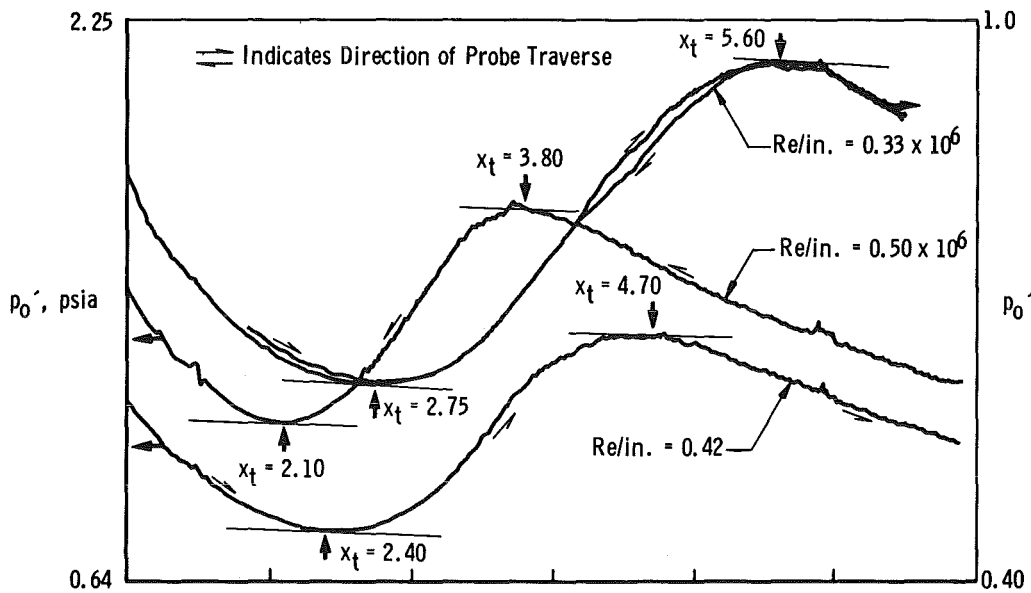
b. Probe No. 1, $M_\infty = 4$, $\Lambda = 50$ deg, $a = 0$
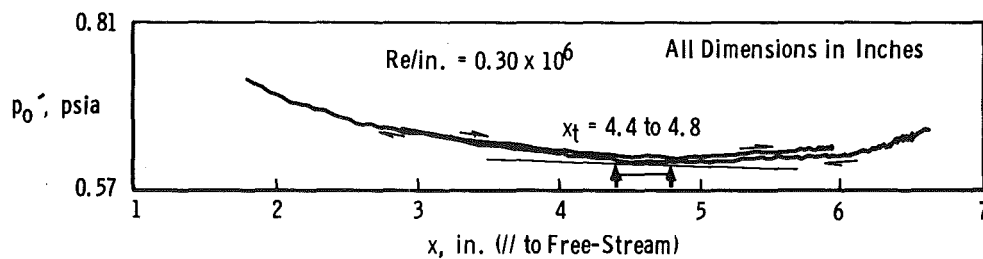
c. Probe No. 2, $M_\infty = 5$, $\Lambda = 50$ deg, $a = -4.2$ deg

Fig. 9 Typical Pitot Probe Traces, Circular Arc Profile

a. Probe No. 1

b. Probe No. 2
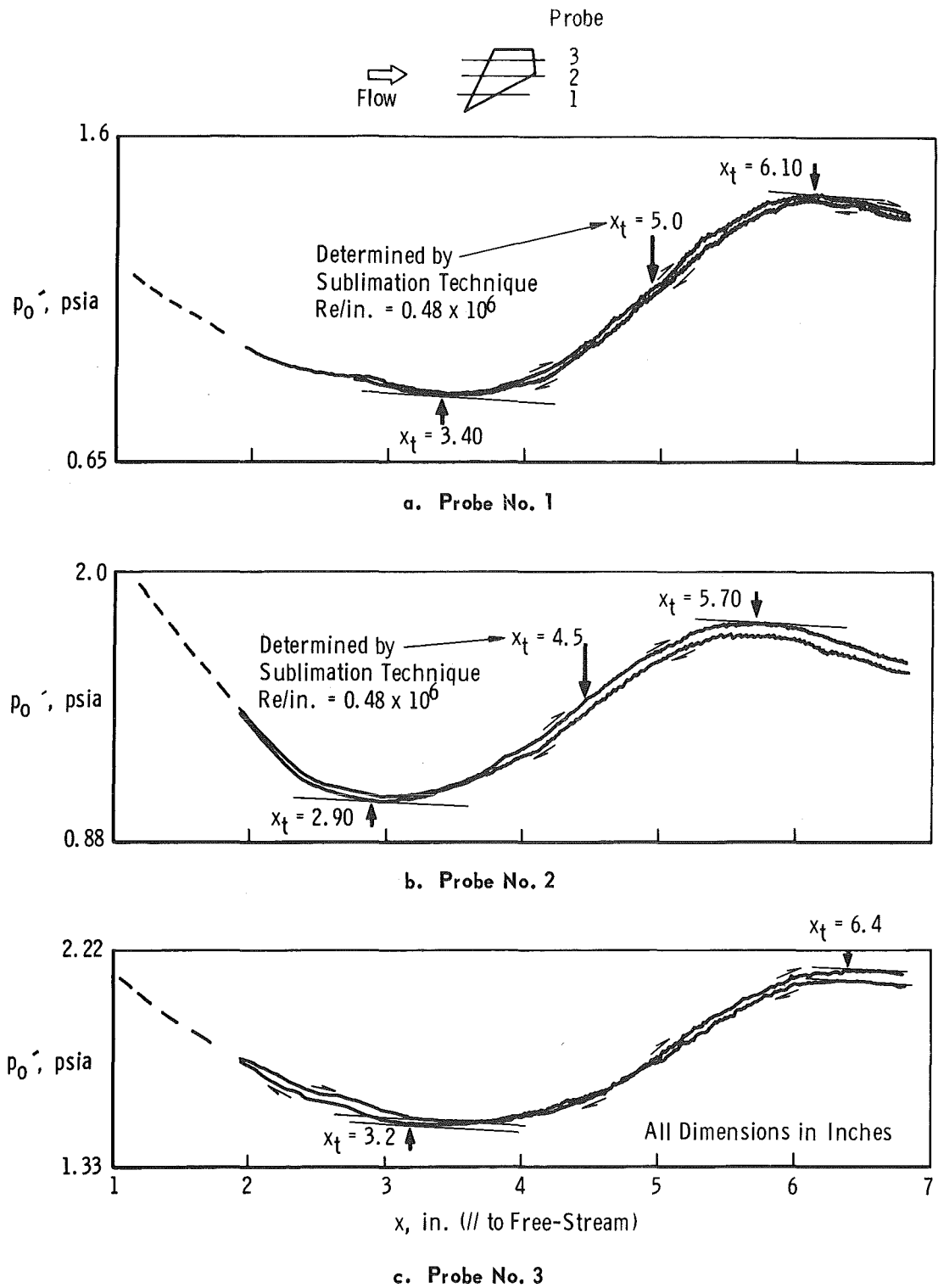
c. Probe No. 3

Fig. 10 Pitot Probe Pressure Traces for Probes No. 1, 2, and 3 at M_∞ = 4, Λ = 36 deg, α = 0, Re/in. = 0.47 x 10^6, Circular Arc Profile

24
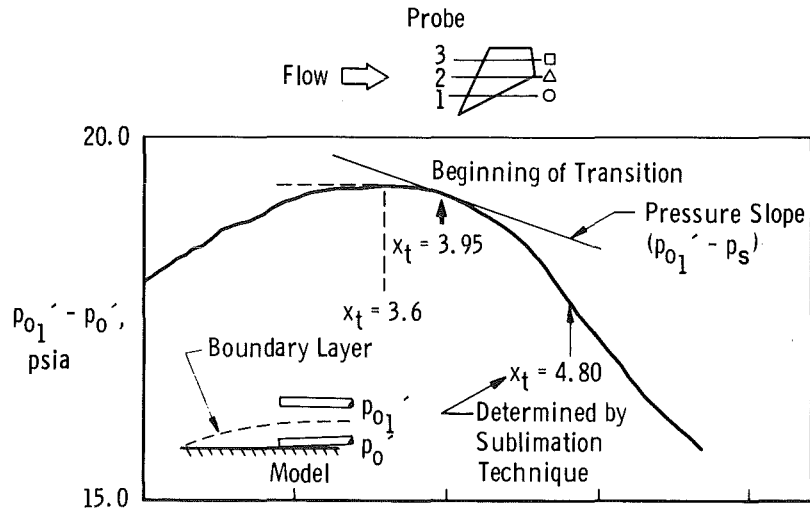
a. Probe No. 3, Pitot Pressure Trace with Pitot Pressure (p_{o_1}') Reference, Re/in. = 0.62 x 10^6
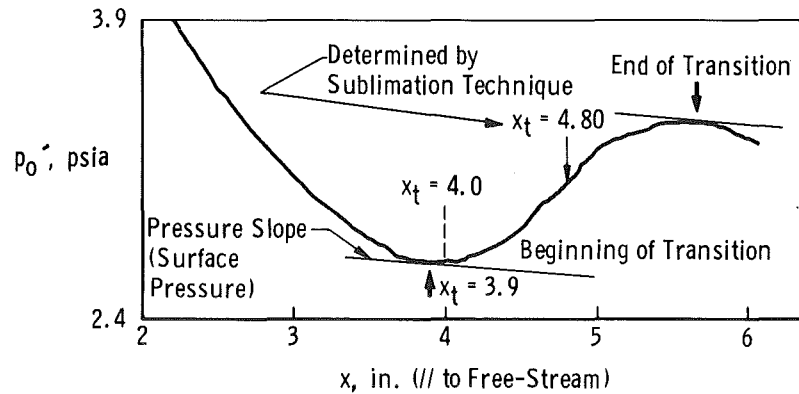
b. Probe No. 3 Pitot Pressure Trace with Vacuum Reference, Re/in. = 0.62 x 10^6
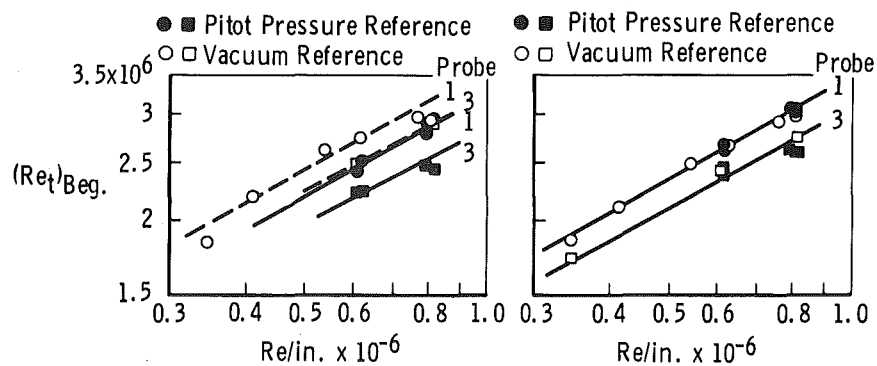
c. Beginning-of-Transition Reynolds Numbers Determined without Slope Correction

d. Beginning-of-Transition Reynolds Numbers Determined with Slope Correction

Fig. 11 Effect of Pressure Slope on Determining Transition Location, M_∞ = 3, Λ = 24 deg α = 0, Circular Arc Profile

a. $M_\infty = 2.5$, $\alpha = 0$

b. $M_\infty = 2.5$, $\alpha = -4.2$

c. $M_\infty = 3$, $\alpha = 0$

d. $M_\infty = 3$, $\alpha = -4.2$
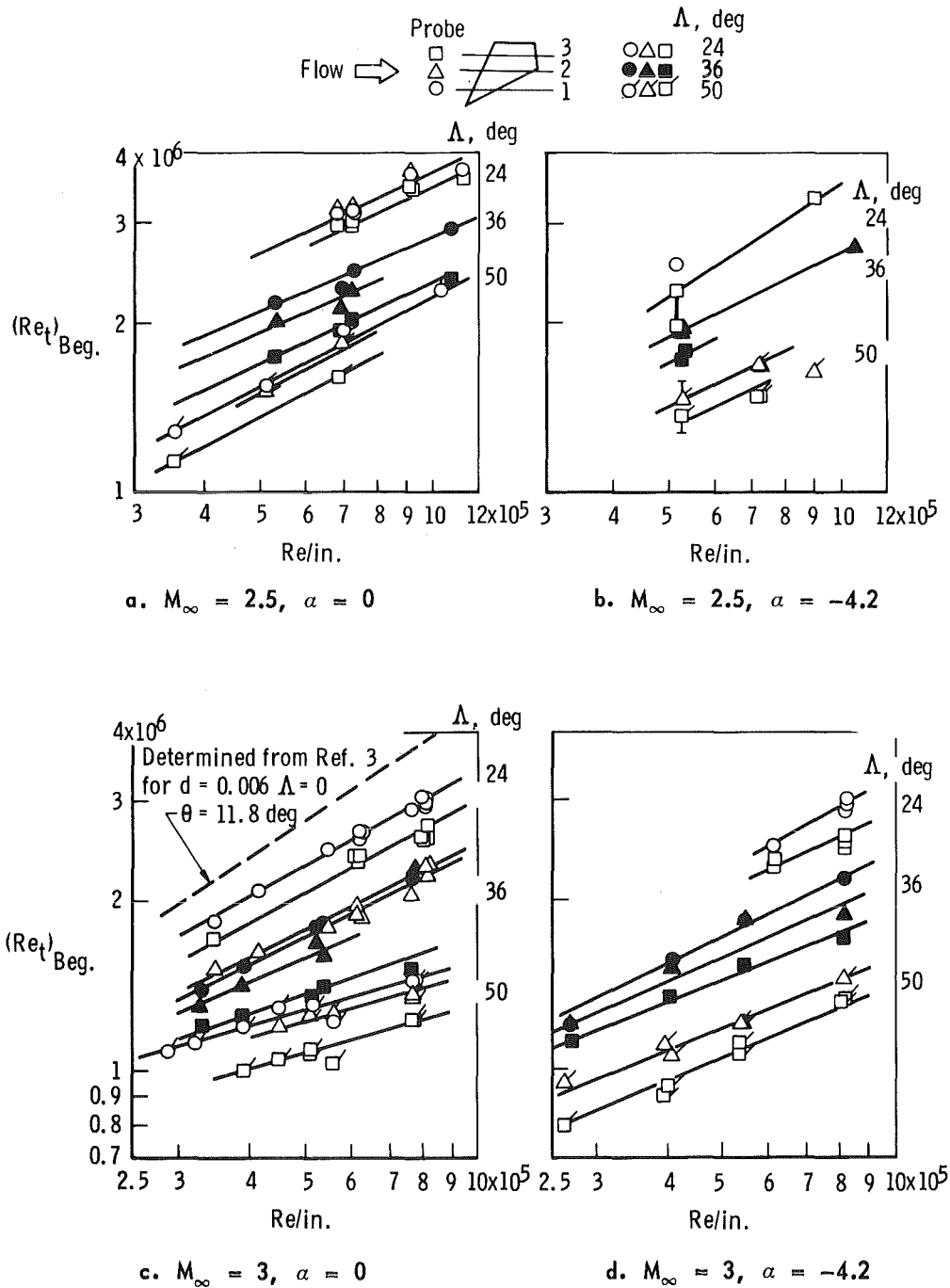
Fig. 12 Beginning-of-Transition Results for $\Lambda = 24$, 36, and 50 deg, $\alpha = 0$ and -4.2 deg at $M_\infty = 2.5$ to 5, Circular Arc Profile

e. $M_\infty = 4$, $\alpha = 0$

f. $M_\infty = 4$, $\alpha = -4.2$

g. $M_\infty = 5$, $\alpha = 0$

h. $M_\infty = 5$, $\alpha = -4.2$

Fig. 12 Concluded

27

a. $M_\infty = 3$, $\alpha = 0$

b. $M_\infty = 3$, $\alpha = -4.6$

c. $M_\infty = 4$, $\alpha = 0$

d. $M_\infty = 4$, $\alpha = -4.6$
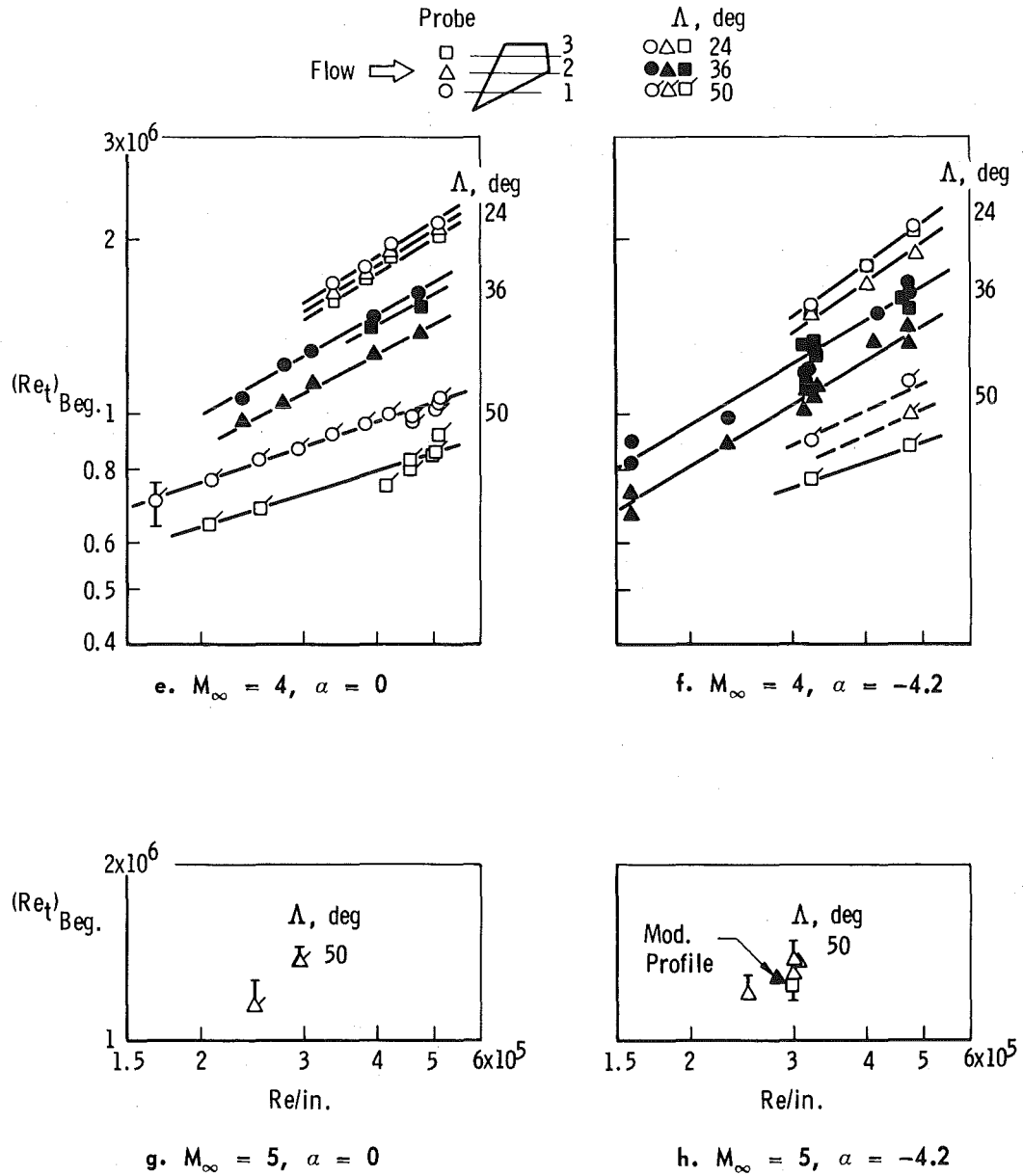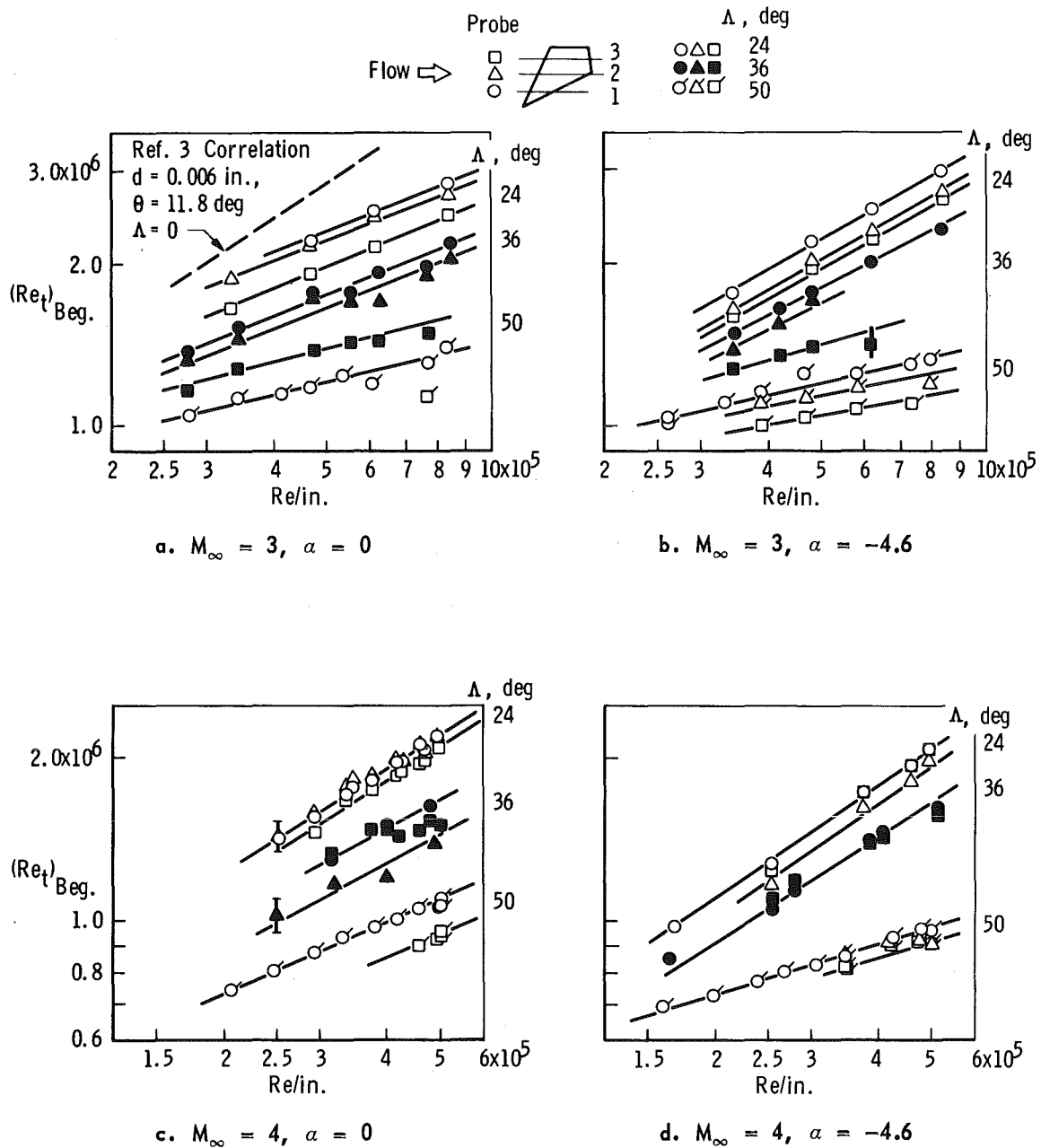
Fig. 13 Beginning-of-Transition Results for $\Lambda = 24, 36$, and 50 deg, $\alpha = 0$ and -4.6 at $M_\infty = 3$ and 4, Modified Arc Profile

a. Beginning of Transition, $M_\infty = 3$

b. End of Transition, $M_\infty = 3$

c. Beginning of Transition, $M_\infty = 4$

d. End of Transition, $M_\infty = 4$
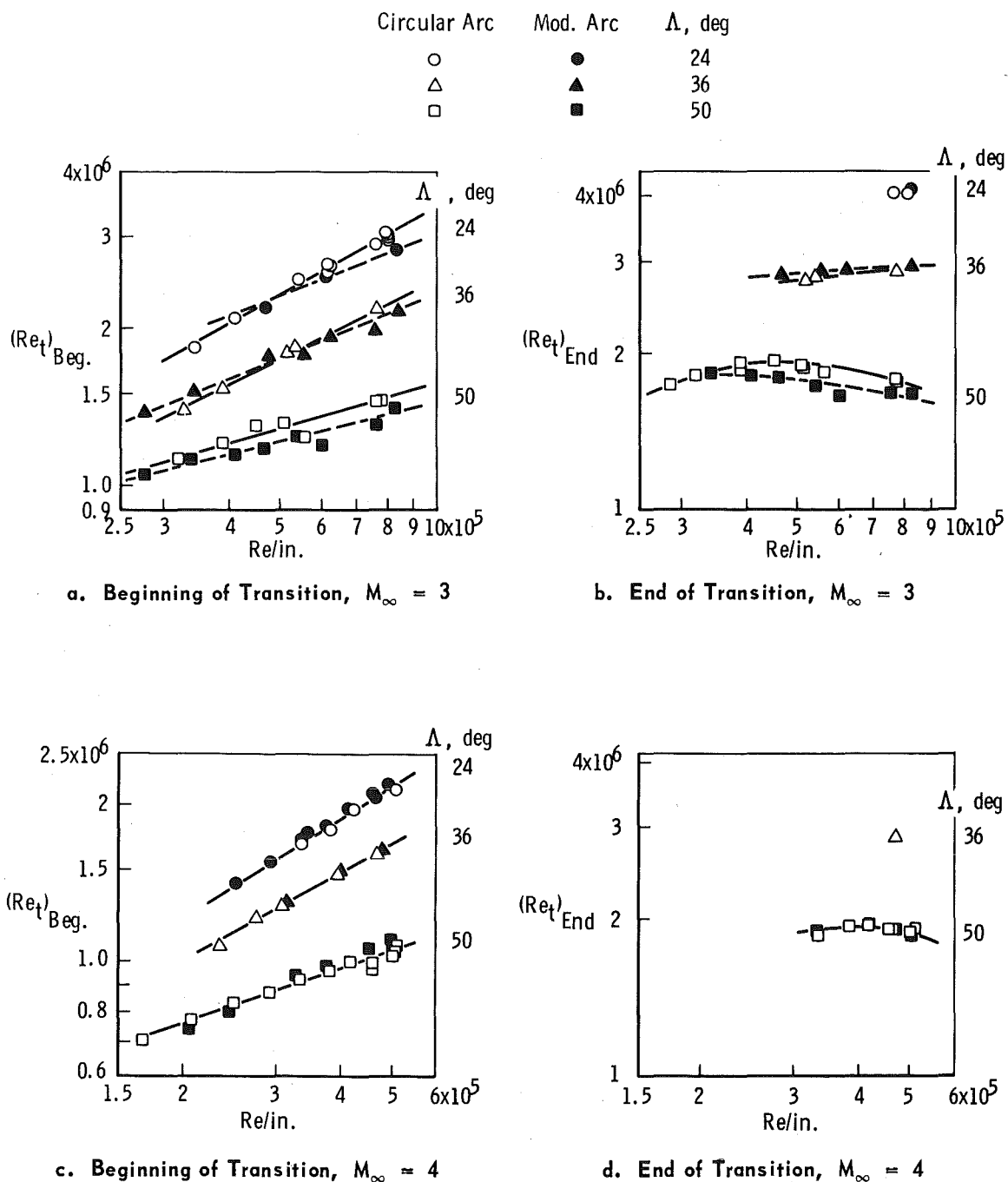
Fig. 14 Comparison of Beginning- and End-of-Transition Data for Circular Arc and Modified Arc Profile, Probe No. 1, $M_\infty = 3$ and 4, $\alpha = 0$

29
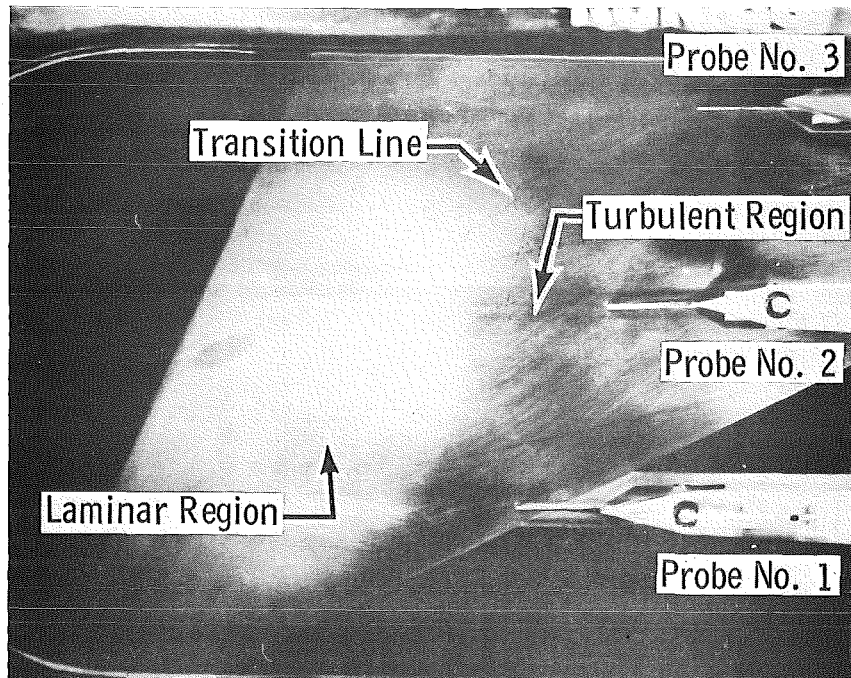
a. Photograph Taken with Tunnel Operating
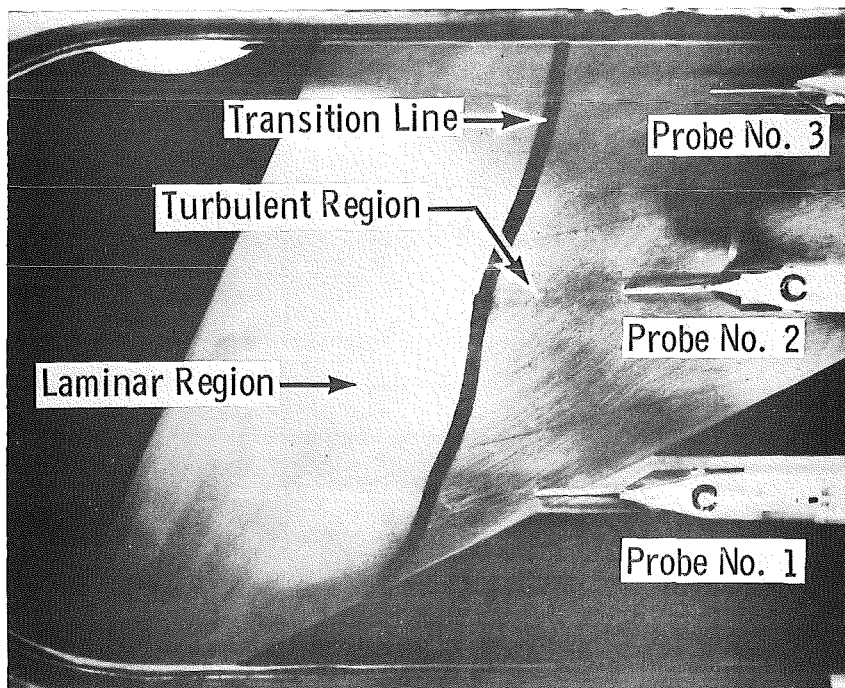
b. Transition Location Indicated by Ink

Fig. 15 Transition as Indicated by the Sublimable Solid for M_∞ = 3, Λ = 24 deg, α = 0, and Re/in. = 0.81 x 10^6, Circular Arc Profile
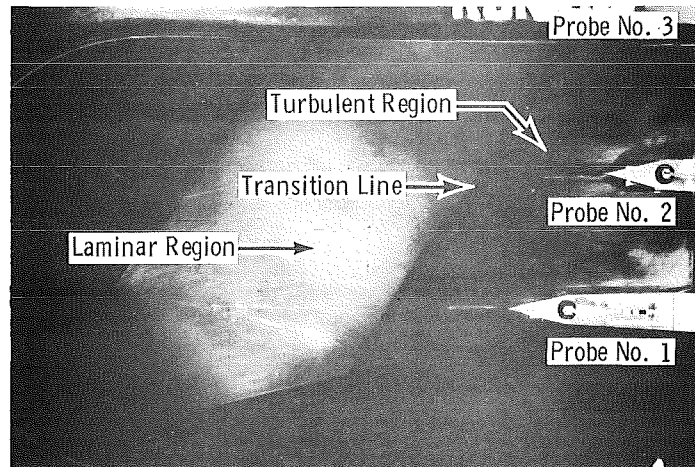
a. $\Lambda = 36$ deg, Re/in. $= 0.27 \times 10^6$
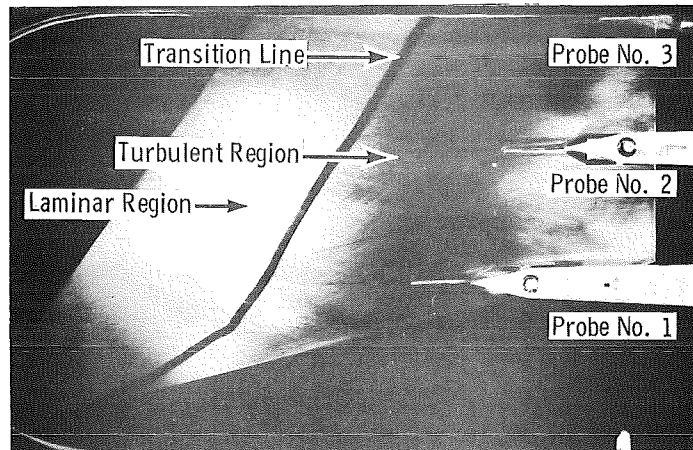
b. $\Lambda = 36$ deg, Re/in. $= 0.54 \times 10^6$
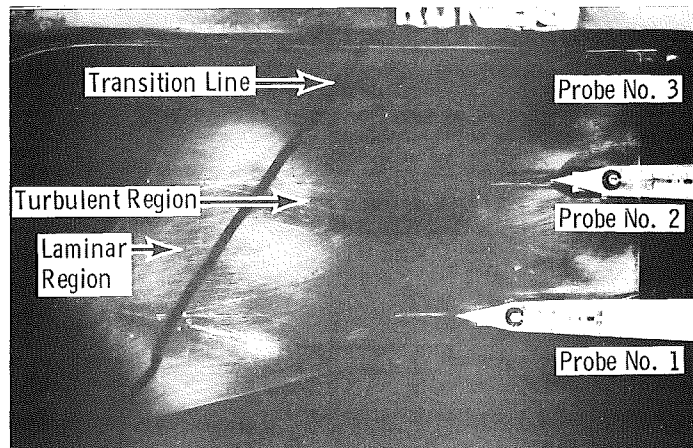
c. $\Lambda = 36$ deg, Re/in. $= 0.81 \times 10^6$

Fig. 16 Photographs Showing the Effect of Unit Reynolds Number on Transition at $M_\infty = 3$, $\Lambda = 36$ and 50 deg, $\alpha = 0$ as Determined by the Sublimable Solid, Circular Arc Profile
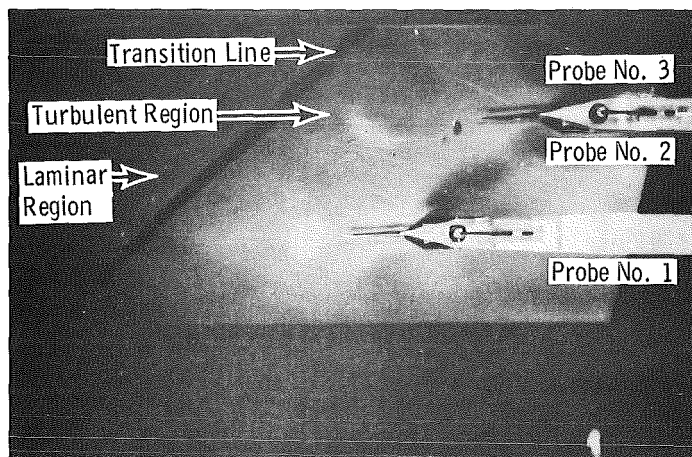
d. $\Lambda = 50$ deg, Re/in. $= 0.41 \times 10^6$
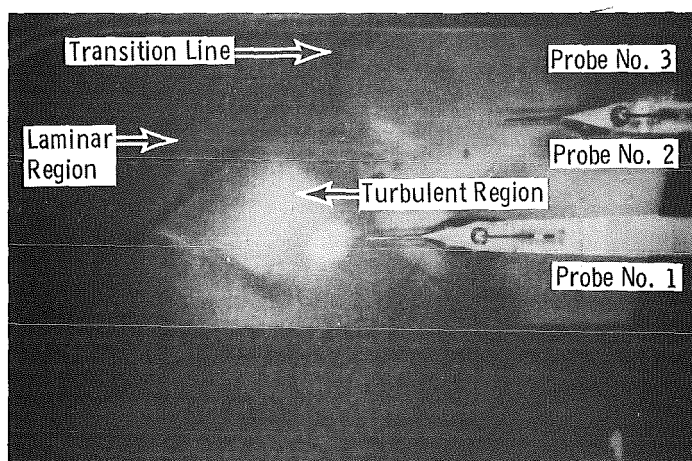
e. $\Lambda = 50$ deg, Re/in. $= 0.81 \times 10^6$

Fig. 16 Concluded
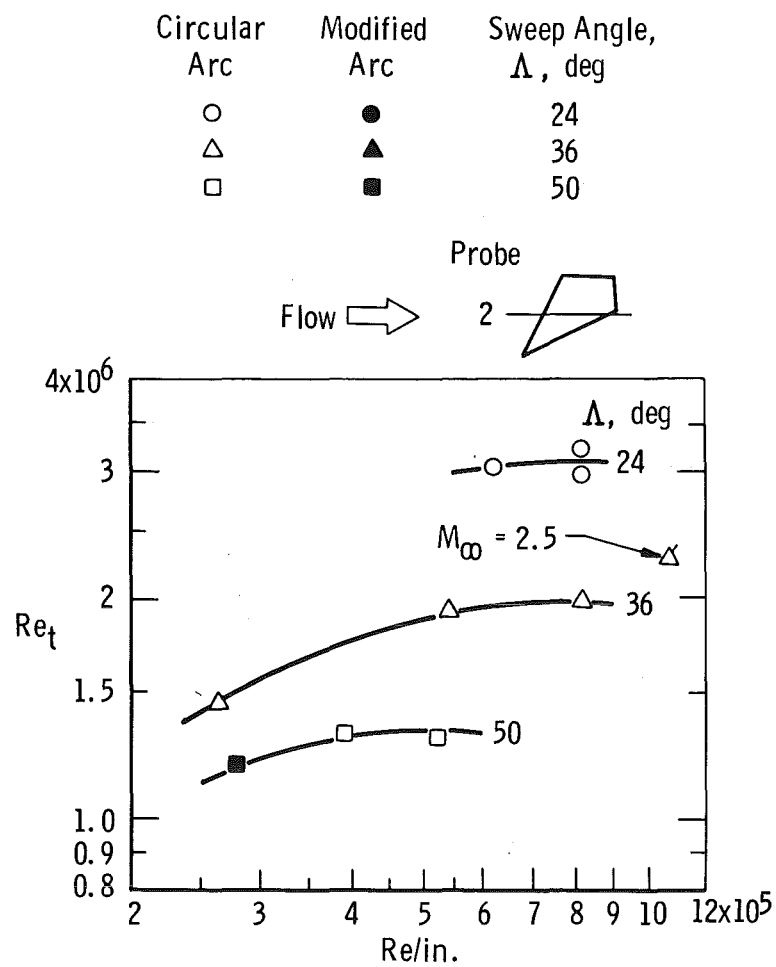
a. $M_\infty = 2.5$ and 3, $\alpha = 0$
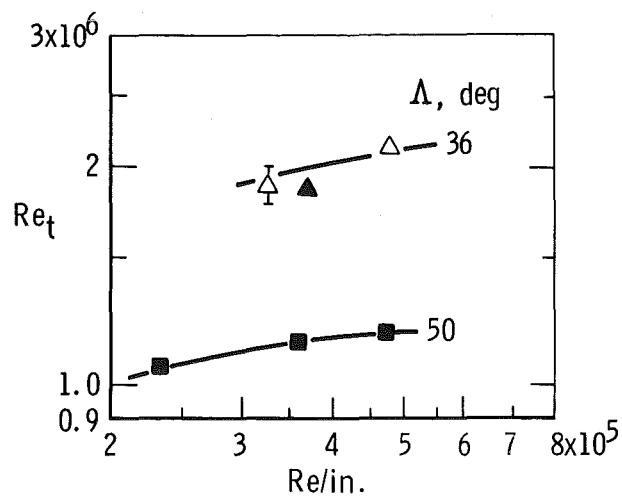
b. $M_\infty = 4$, $\alpha = 0$

Fig. 17 Transition Results Obtained by Sublimation Technique
at Probe No. 2 Location and $M_\infty = 2.5$ to 4, $\alpha = 0$
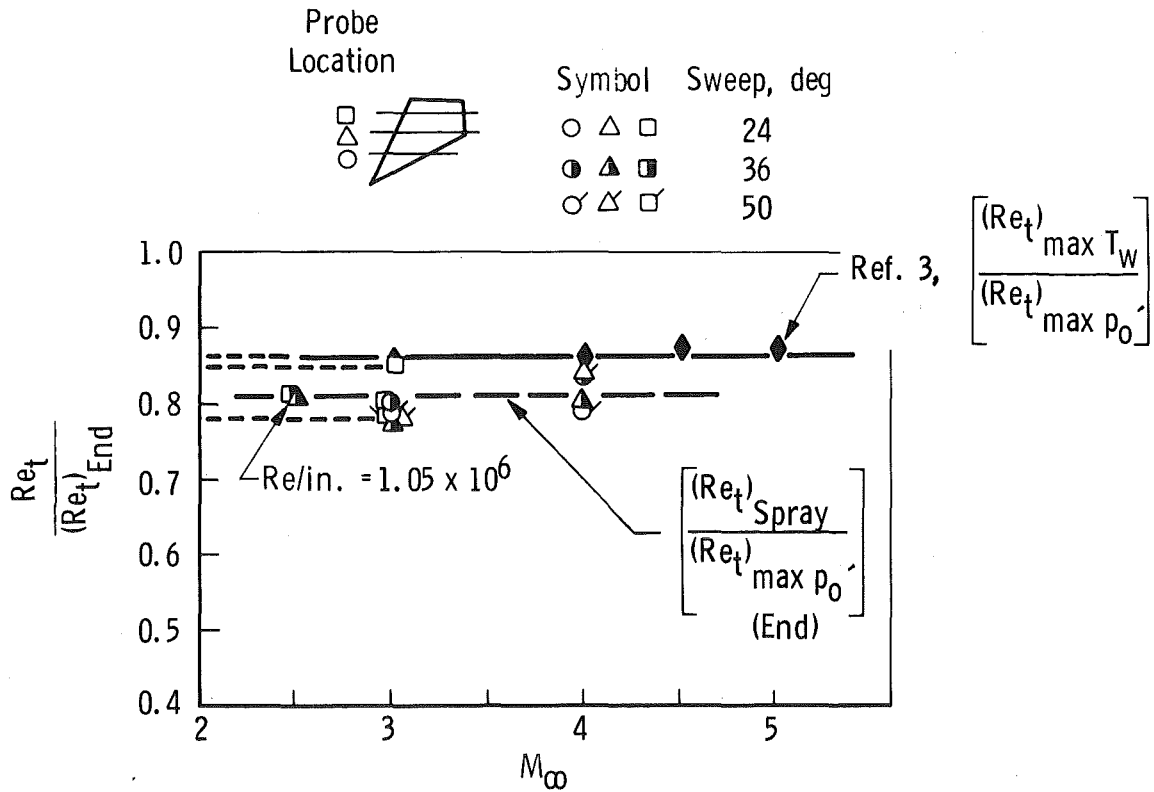
a. Transition Results from Various Indicators, Re/in. = 0.50 x 10^6
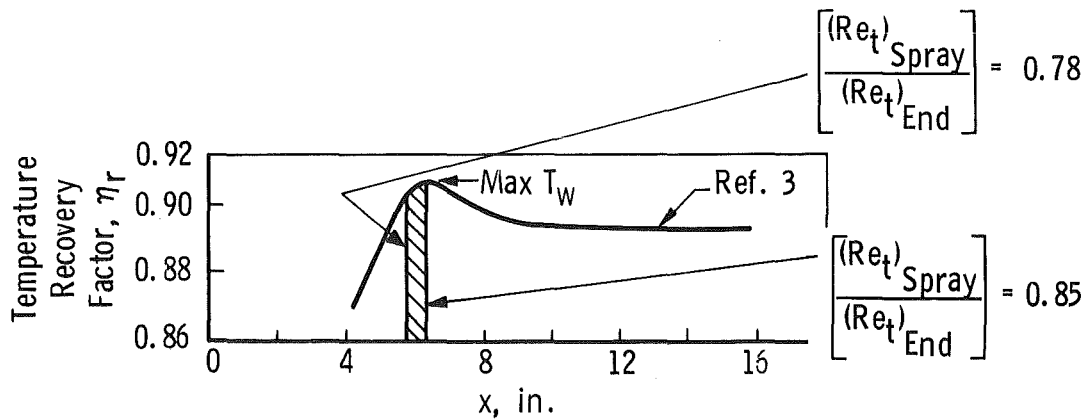
b. Surface Temperature Recovery Profile for M_∞ = 3.5, Re/in. = 0.27 x 10^6

Fig. 18 Comparison of Transition Results from Various Methods, α = 0

a. Λ = 24 deg

b. Λ = 36 deg

c. Λ = 50 deg
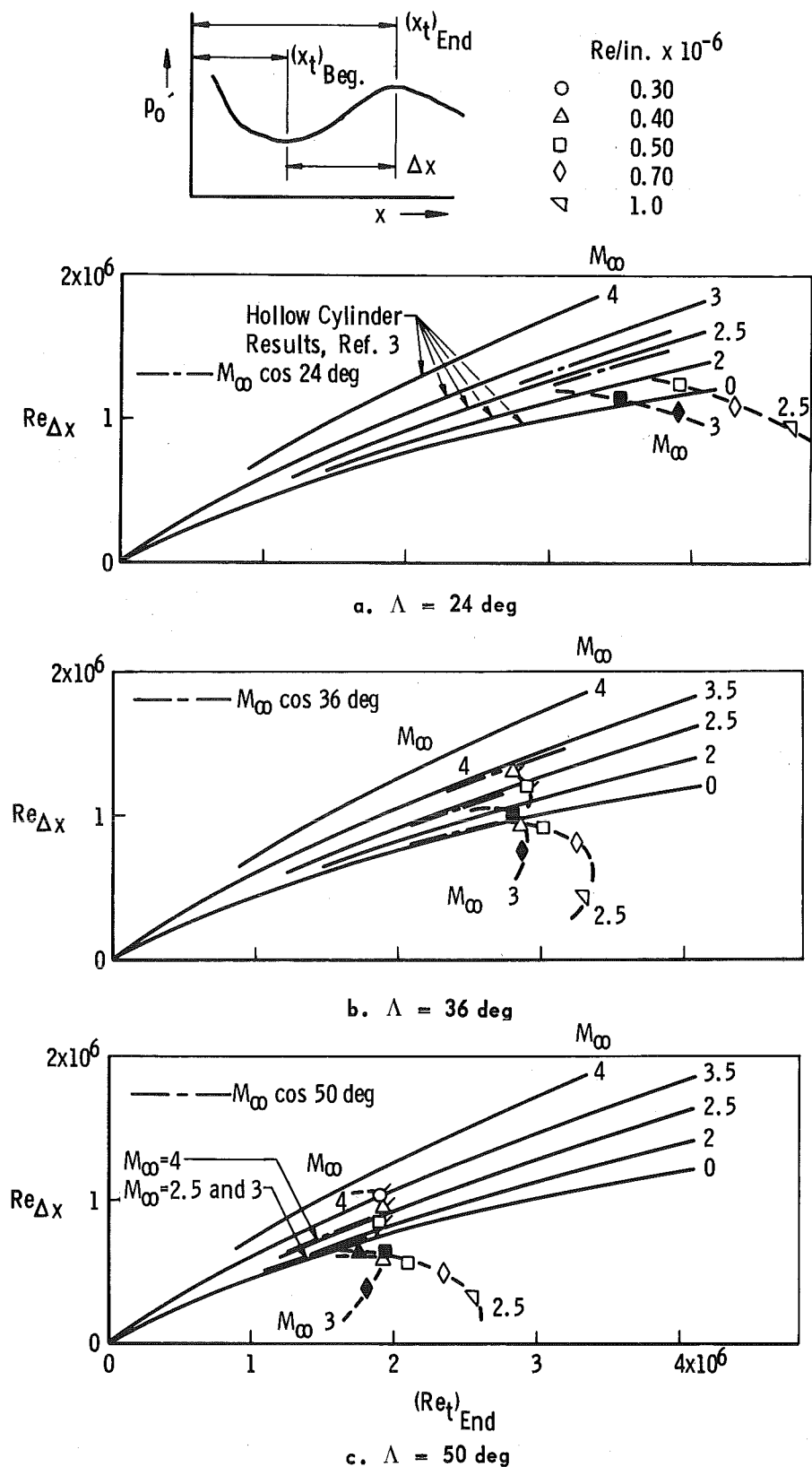
Fig. 19 Reynolds Number Based on Transition Region Length, Probe No. 1, Circular Arc Profile

Flagged Symbols Represent Modified Arc Profile

Unflagged Symbols Represent Circular Arc Profile

a. Beginning of Transition

b. End of Transition
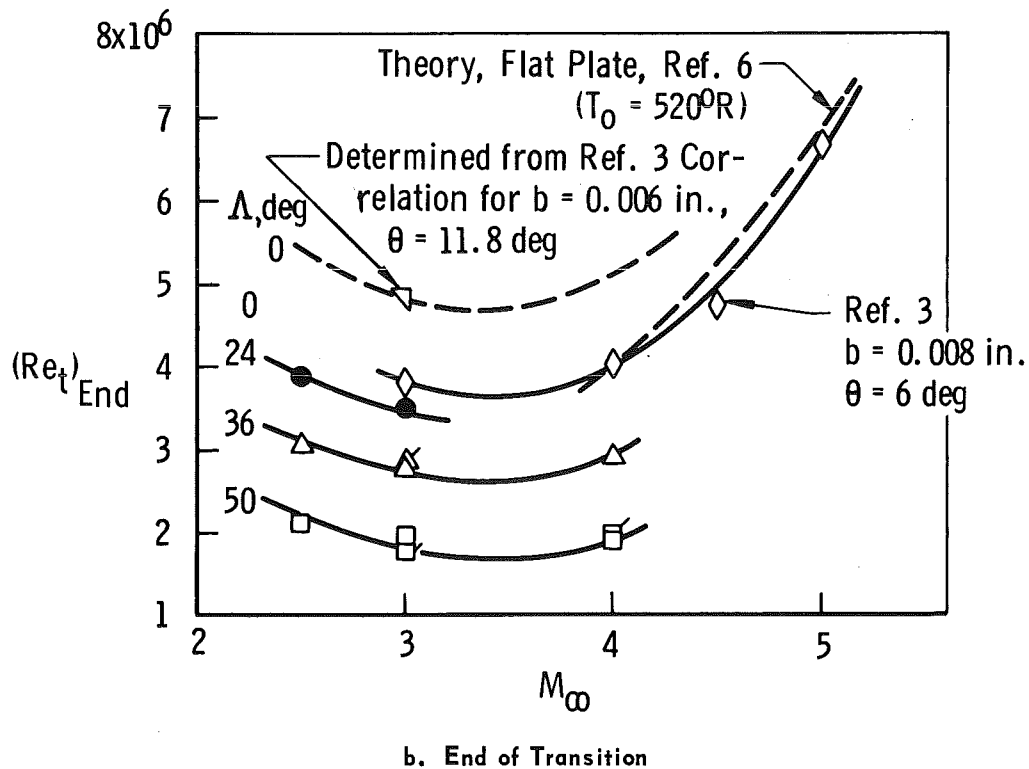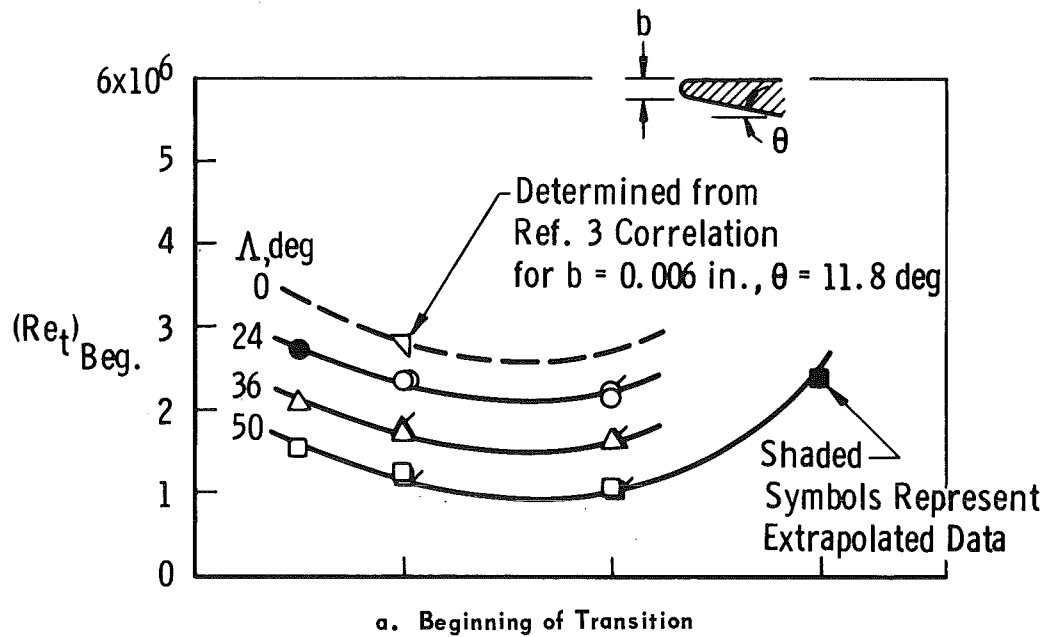
Fig. 20 Variation in Transition Reynolds Number with Mach Number and Sweep Angle for Re/in. = 0.50 x 10^6, Probe No. 1, $\alpha = 0$
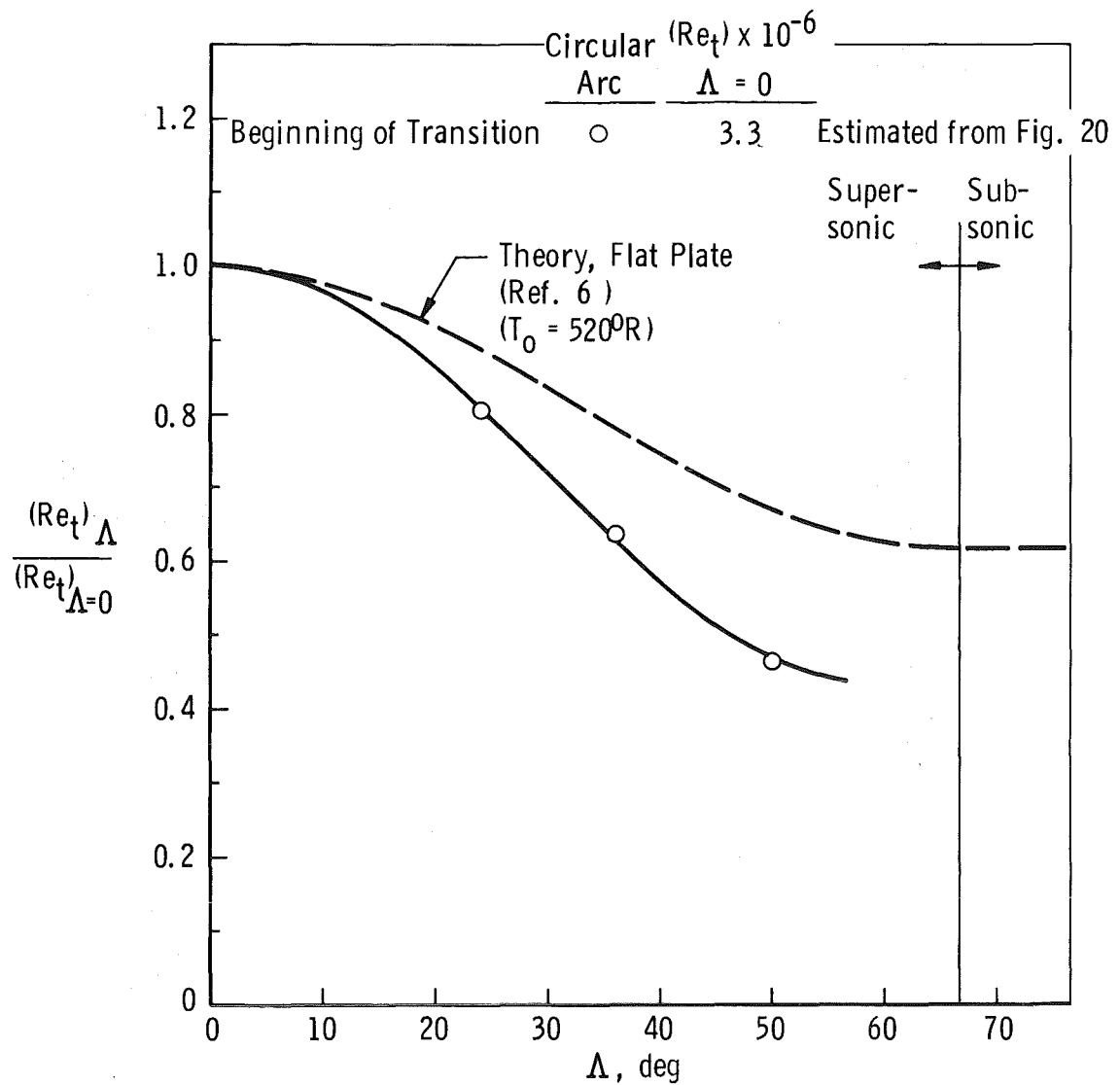
a. $M_\infty = 2.5$, Probe No. 1

Fig. 21 Effect of Sweep on Normalized Transition Reynolds Number for Re/in. = 0.50 x 10^6 and Mach Numbers 2.5, 3, and 4, $\alpha = 0$
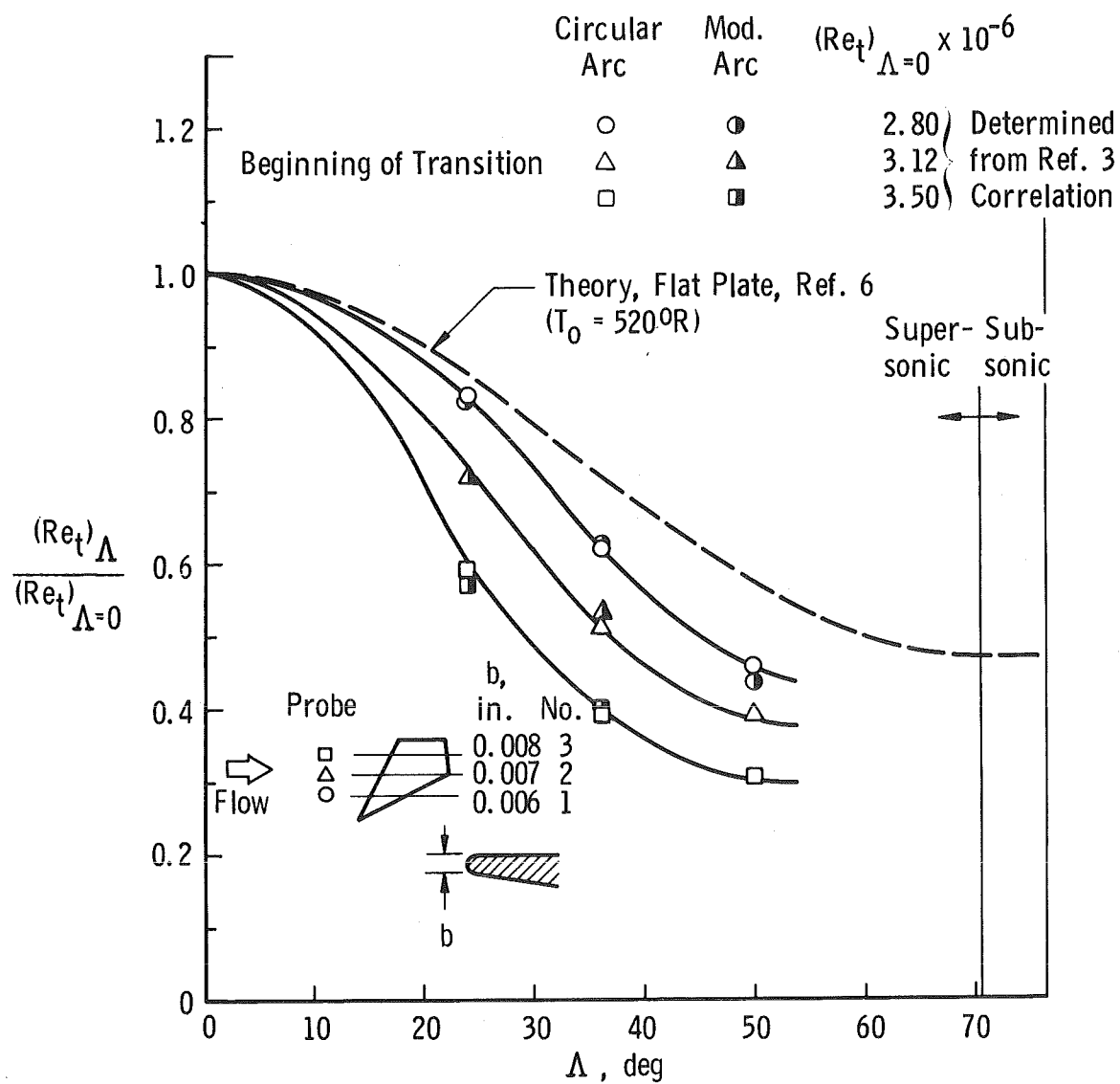
b. $M_\infty = 3$, Probe No. 1, 2, and 3

Fig. 21 Continued
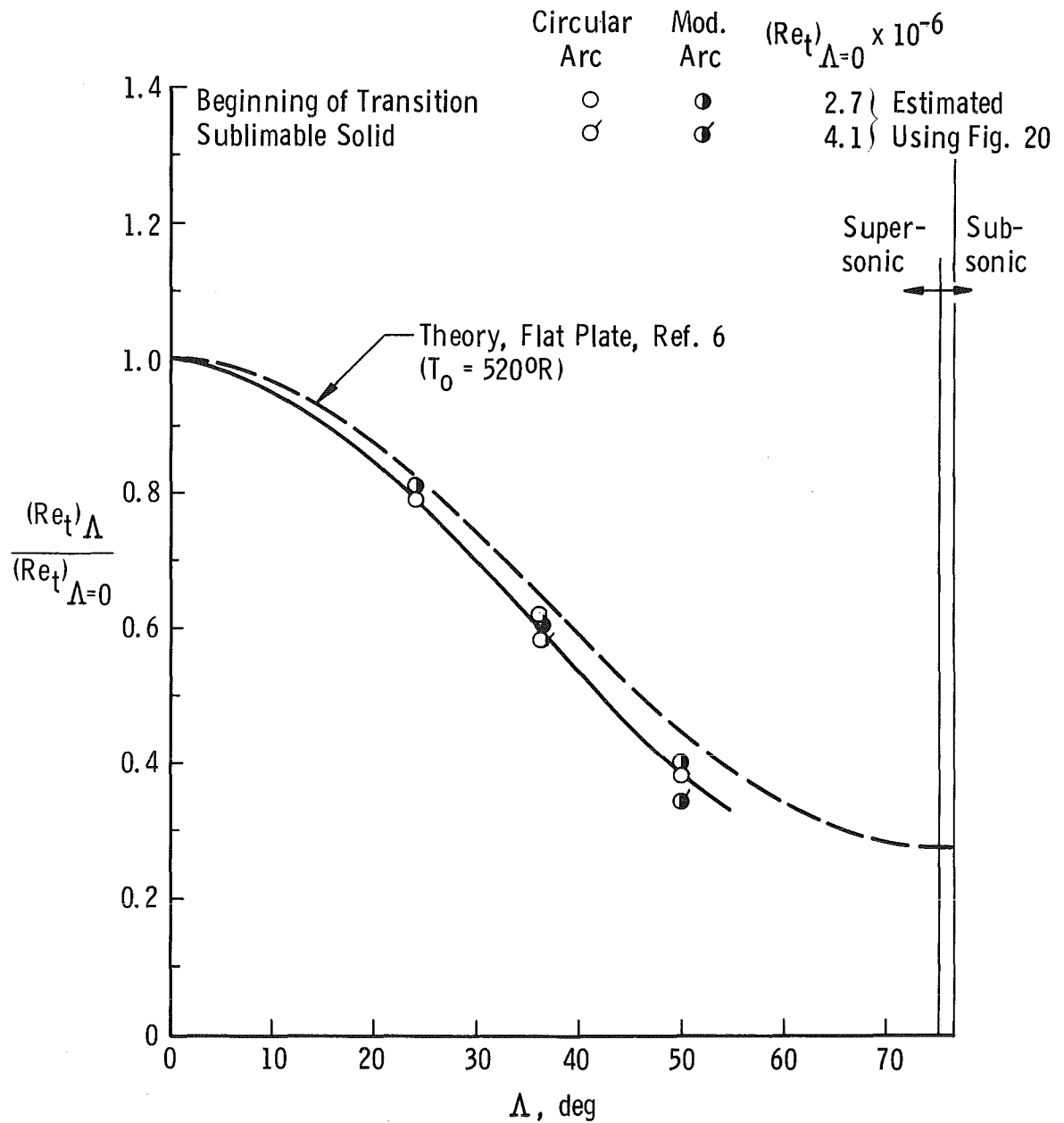
c. $M_\infty = 4$, Probe No. 1 Location

Fig. 21 Concluded
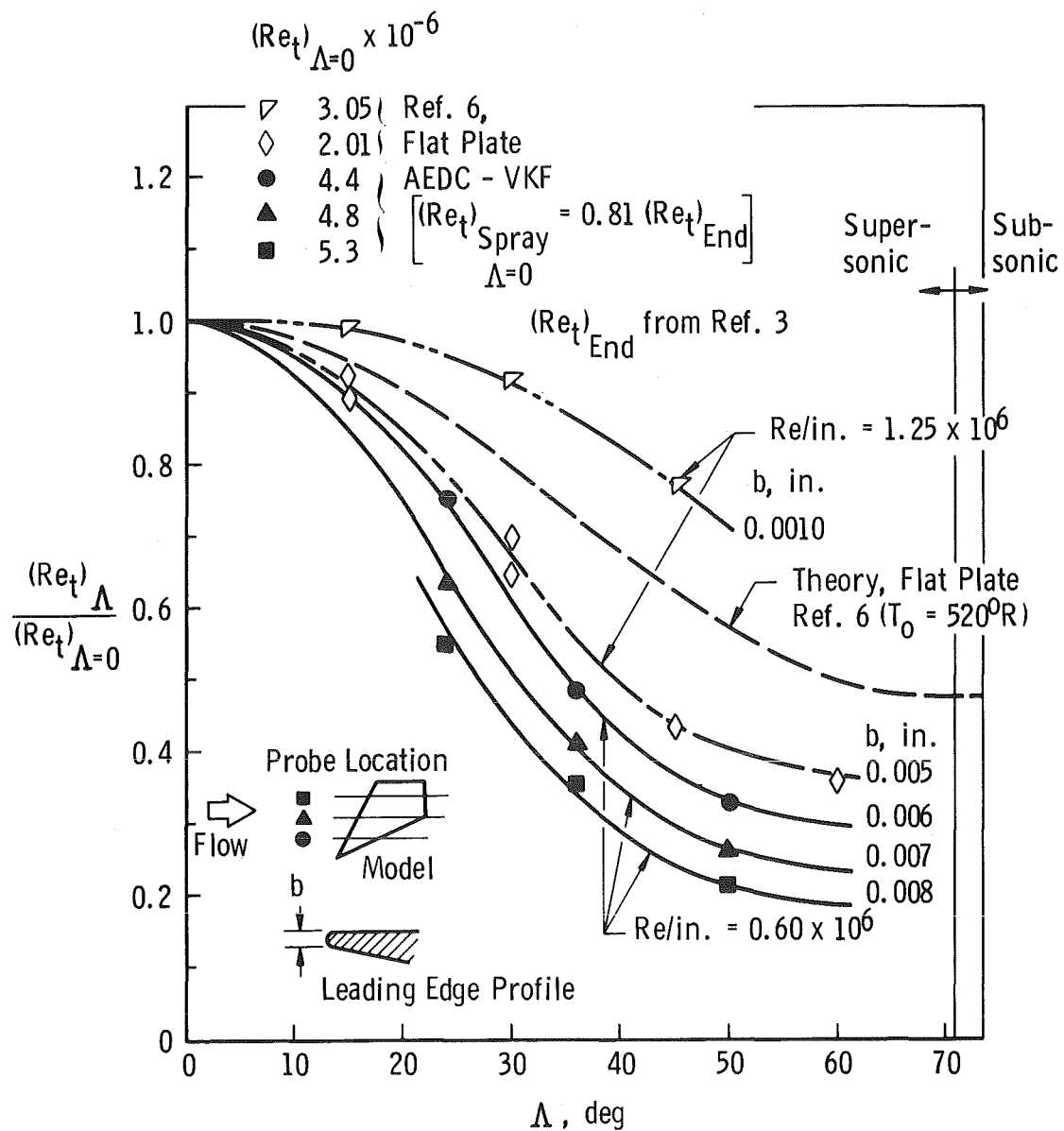
Fig. 22 Variation in Normalized Transition Reynolds Number with Sweep and Spanwise Location at $M_\infty = 3$, $\alpha = 0$, Re/in. $= 0.60 \times 10^6$ as Determined by a Sublimable Solid, Circular Arc Profile
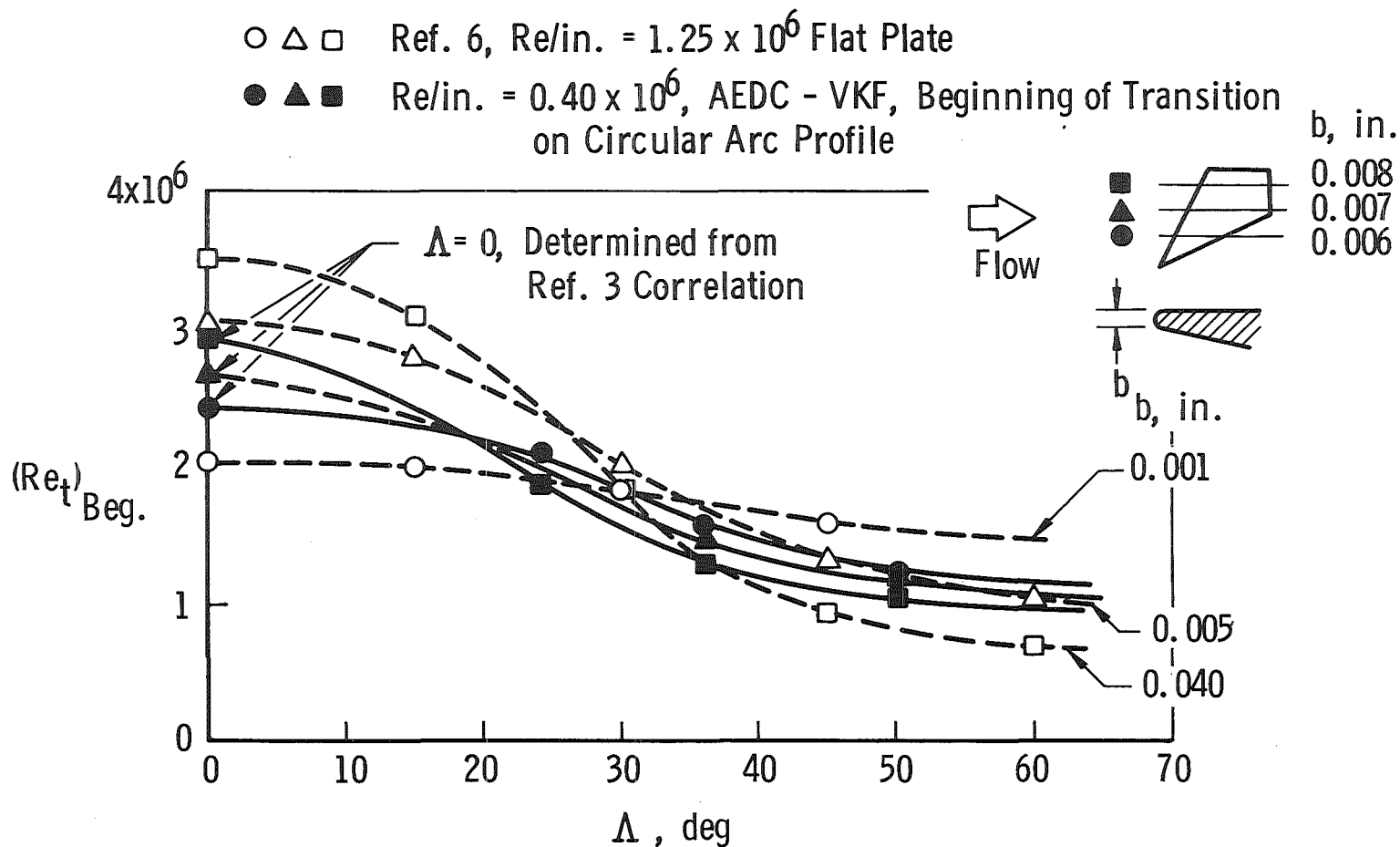
Fig. 23 Effect of Sweep Angle and Leading Edge Thickness on Transition at $M_\infty = 3$, $\alpha = 0$

Arnold Engineering Development Center
Arnold Air Force Station, Tennessee
Rpt. No. AEDC-TDR-63-109. INVESTIGATION OF
BOUNDARY-LAYER TRANSITION ON SWEPT WINGS AT
MACH NUMBERS 2.5 TO 5. July 1963. 51 p. incl 11 refs.
illus.
Unclassified Report

Tests were conducted in the 12-in. Supersonic Tunnel of
the von Kármán Gas Dynamics Facility to determine
boundary-layer transition locations on swept wings having
a circular arc profile and modified arc profile. Test Mach
numbers were from 2.5 to 5 over a Reynolds-number-per-
inch range from 0.14 to 1.08 million at sweep angles of
24, 36, and 50 deg for angles of attack of 0 and approxi-
mately -4 deg. Boundary-layer transition Reynolds num-
bers determined by a pitot probe, and results obtained
visually with a sublimable solid are presented. The major
factors influencing boundary-layer transition were wing

sweep and model leading edge geometry. Increasing wing
sweep and leading edge bluntness above a sweep angle of
approximately 20 deg decreased the transition Reynolds
number at all test Mach numbers.

1. Swept wings
2. Boundary-layer transition
3. Supersonic characteristics
I. AFSC Program Area 750A,
   Project 1366, Task 136612
II. Contract AF 40(600)-1000
III. ARO, Inc., Arnold AF Sta,
   Tenn.
IV. S. R. Pate and
   R. E. Brillhart
V. Available from OTS
VI. In ASTIA Collection